



Diagnostic Imaging in the Degenerative Diseases of the Cervical Spine

Giuseppe Maria Di Lella,
Alessandro Maria Costantini, Edoardo Monelli,
Giulia Guerri, Antonio Leone,
and Cesare Colosimo

Introduction

Degenerative changes of the cervical spine, both physiological and pathological, proceed jointly with the age and can be easily identified and characterized by modern radiological techniques. The aging of the cervical spine, in particular, involves all its structures (osteo-discal-ligamentous complex); however, the intervertebral joints are the earlier and more conspicuously involved targets, being also the most specifically linked to the symptoms determined by the involution process [1]. Imaging can also distinguish degenerative diseases from other causes of radiculo-miopathy, (i.e. infection or neoplasms).

In this scenario, magnetic resonance imaging certainly represents the best imaging modality in the evaluation of degenerative disease, especially in the cervical segment, where other methods of investigation (radiography, computed tomography) do not have a high diagnostic accuracy because of the peculiar anatomical features of the

cervical spine. However, imaging findings must be considered clinically relevant only if correlated to the patient's symptomatology, as degenerative changes of the cervical spine can be easily found in asymptomatic patients older than 30 years [2]. In fact, imaging findings alone do not justify an aggressive therapy, particularly because some acute soft disk herniations can significantly decrease in size over time with conservative therapy [3]. This chapter is an attempt to help the clinician with a daily imaging reference in the treatment and management of patients with cervical spine degenerative disease.

Basic Anatomy

Two anatomically and functionally distinct components could be recognized in the cervical spine. The upper cervical spine (or suboccipital spine) consists of the first two cervical vertebrae, atlas and axis, articulating with the occipital bone, forming the craniocervical junction (CCJ). The lower cervical spine (or subaxial cervical spine) extends from the C2–3 to the C7–T1 joints [4].

Cranio-Cervical Junction

The atlas is ring-shaped; it is formed by a thick anterior arch, a thin posterior arch, two lateral masses, and two transverse processes. In the transverse process there is a foramen, through

G. M. Di Lella (✉) · A. M. Costantini · E. Monelli
G. Guerri · A. Leone · C. Colosimo
Department of Radiological Sciences, Radiology/
Neuroradiology Institute, Catholic University of
Sacred Heart, Polyclinic A. Gemelli, School of
Medicine, Rome, Italy
e-mail: giuseppemaria.dilella@unicatt.it;
marialuigia.angeli@policlinicogemelli.it;
alessandro.costantini@policlinicogemelli.it;
alessandro.pedicelli@policlinicogemelli.it;
colosimo@rm.unicatt.it;
cesare.colosimo@policlinicogemelli.it

which passes the vertebral artery (transverse foramen). Lateral masses have a superior and an inferior articular facet which form the zygapophyseal joint.

The axis is composed by the vertebral body (which contains the odontoid process), large pedicles, laminae, and transverse processes; the odontoid process has an anterior articular facet that articulates with the anterior arch of the atlas.

The craniocervical junction includes six synovial joints: a pair of atlo-occipital joints, the anterior and posterior atlo-odontoid joint and a pair of atlo-axial lateral joints. The atlo-occipital joints are determined by the effacing between the occipital condyles and the superior articular facets of the atlas. The atlo-odontoid joint takes place between the dens and a osteofibrous ring formed by the frontal arc of the atlas and the transverse ligament. The atlo-axial lateral joints articulate the facet joints of the axis and of the atlas.

The craniocervical junction is held in place by extrinsic and intrinsic ligaments. The extrinsic ligaments include the nuchal ligament, which extends from the external occipital protuberance to the posterior portion of the atlas and of the cervical spinous processes and fibroelastic membranes that replace the anterior longitudinal ligament, intervertebral disks and the flaval ligaments.

The intrinsic ligaments, located within the spinal canal, provide the majority of joint stability. From the dorsal to the ventral side, they include the tectoria lmembrane, the cruciate ligament and the odontoid ligaments (apical and alar ligaments). The tectorial membrane connects the back of the axis body to the front of the foramen magnum and represent the cephalic continuation of the posterior longitudinal ligament. The cruciate ligament lies anterior to the tectorial membrane, behind the odontoid process; it is formed by longitudinal fibers, which extend from the anterior margin of the foramen magnum to the body of the axis, and by the transverse ligament, a sturdy fibrous tape stretched between the internal surfaces of the atlas masses. A synovial cavity is located between the dens and the transverse

ligament. The transverse ligament is the most important ligament to avoid abnormal anterior translation. Odontoid ligament secure the axis dens to the occipital bone through the apical ligament and two alar ligaments, which prevent excessive lateral and rotational motion [5].

Subaxial Cervical Spine

Subaxial cervical spine includes vertebrae C3–C7. Vertebral bodies are concave on their superior surface and convex inferiorly. On the superior surfaces of the bodies arise processes, or hooks, called uncinat processes, each of which articulates with a depression on the inferior endplate of the superior vertebral body (Luschka joints, not considered true articulations) [6]. In most cases the spinous processes of C3–6 are bifid, while the spinous process of C7 is not.

Each vertebra has two superior and two inferior zygapophyseal joints, a disco-somatic joint and two, as we have just mentioned, Luschka joints. The facet joints are diarthrodial synovial joints with fibrous capsules.

The anterior longitudinal ligament (ALL) and the posterior longitudinal ligament (PLL) are found throughout the entire length of the spine; the former is not well developed in the cervical spine and is more closely adherent to the disks than the latter. ALL and PLL are the caudal extension, respectively, of the anterior atlanto-occipital membrane and of the tectorial membrane in the lower cervical spine. The supraspinous ligament, the interspinous ligaments, and the flaval ligaments (posterior ligamentous complex) maintain stability between the vertebral arches. The flaval ligament is the most important: runs from the anterior surface of the cephalic vertebra to the posterior surface of the caudal vertebra and, aided by the interspinous ligament, control the excessive flexion and anterior translation. The flaval ligament also connects to and reinforces the facet joint capsules on the ventral aspect.

Intervertebral disks are located between the vertebral bodies between C2 and C7 and are

made of four parts: the nucleus pulposus, the annulus fibrosus and two endplates attached to the superior and inferior vertebral bodies. The disks are thicker anteriorly: with the physiological process of aging the disks become progressively dehydrated and show height reduction.

The foramina progressively decrease in size from C2–3 to C6–7; the spinal nerve, which is the result of the union of the anterior and posterior nerve roots, occupy about one third of the foraminal space. The foramen is bordered anteriorly by the uncovertebral joints, posterolaterally by facet joints, superiorly by the pedicle of the vertebra above, and inferiorly by the pedicle of the underlying vertebra.

Technical Approach

Diagnostic workup in the assessment of degenerative cervical spine disease has the aim to identify the pathology of the spinal osteo-discal-ligamentous complex (i.e. spondylosis, hernias, etc.) and the consequently determined alterations of the “content” (spinal cord). We will briefly describe the most important imaging modalities (radiography, computed tomography, magnetic resonance imaging) in the evaluation of the effects of degenerative diseases that should be considered in advance to any therapeutic planning [7].

Radiography

Even if radiography is considered the “first step” technique in the study of degenerative cervical spine examination, nowadays it has undergone critical re-evaluation and its role is currently controversial [8, 9]. In the assessment of brachialgia, radiography can only provide information about the degenerative changes of bone spinal structure, but it is limited in the evaluation of stenosis of the central canal and disk herniation, the most frequent causes of pain and neurologic symptoms. The only indisputable use of radiography is confined to assessment of the instability, performing a flexion-extension radiograms

[10]. However, the functional radiological study itself can't demonstrate the most frequent cause of instability represented by ligament laxity/injury.

Computed Tomography

The introduction of new multidetector computed tomography (CT) scanner has completely changed the accuracy and diagnostic capabilities of CT in the evaluation of degenerative cervical spine disorders. A slice thickness of 0.6–0.7 mm with 1 mm reconstruction and increases of 0.5–0.6 are recommended parameters in order to achieve an optimal visualization of degenerative changes. Contrary to radiography, CT is capable to visualize not only the bony structures but also some soft tissues features (e.g. disk herniations). In the last years the advent of new method of dose optimization, like ASIR (Automated system for Iterative Reconstruction), that could reach up to 50% of dose reduction, made the CT less invasive, especially when studying bone structures. However the overall quality of the images worsen, especially in the evaluation of soft tissues.

CT is inadequate in the study of ligaments and bone marrow changes, which almost exclusively done with MR imaging. Multiplanar and 3D reconstruction may be a useful integration to the axial examination, especially in surgical planning [11]. The use of contrast media nowadays should be strictly limited to the cases in which the Pt is not feasible for an MRI study (i.e. intensely claustrophobic and not willing to do on sedation, bearer of non MRI compatible devices etc.). In every case it is necessary to highlight the absolute uselessness of iodine contrast when evaluating the bone structures: in fact the increase in density provided by contrast media would not change the bone intrinsic hyperdensity. Eventually, iodine could be used, in these Pts, for the differentiation between hernia relapse and granulation tissue. Finally, the most significant limitations of CT results from its inability to demonstrate spinal cord disease, making MRI the modality of choice in patients with clinical evidence of myelopathy.

Magnetic Resonance Imaging

Cervical spine MR examination should be acquired with high-field equipment (≥ 1.5 T), using powerful gradient systems and phased-array coils: with the progressive spreading of the 3T MRI, these systems should be considered as the new gold standard. These images offer several advantages over those obtained on the lower-field scanners, including improved image quality (higher spatial and contrast resolution) and clinical efficiency (higher temporal resolution). However the higher magnetic field lengthen the T1 and T2 relaxation times, with the consequent need to adjust the imaging sequences and, in some ways, the semiotic. These imaging protocols, incorporating the so called “driven equilibrium”, SPACE readout and parallel imaging, have demonstrated its effectiveness in evaluating degenerative disease in the cervical but also in the thoracic and lumbar spine. The combination of high contrast and improved spatial resolution allows the radiologist to characterize disc pathology, assess for presence of cord and nerve root impingement, and evaluate neural foraminal stenosis.

The T1- and T2-weighted (T1-w and T2-w) images in sagittal and axial planes, which represent the baseline examination, should be completed with 2D–3D GRE T2*-w axial and sagittal images, in order to optimize the contrast between the bony and the discal/ligamentous structures. However, in some cases, more specific sequences and scanning planes could be added, to complete the study and optimize the diagnosis (i.e. oblique planes for studying nerve roots course).

Fat-sat sequences, such as fat-suppressed (fat-suppressed T2-weighted [FST2W] or short tau inversion recovery [STIR] should be routinely comprised in every study protocol: they are of paramount importance in evaluating every kind of signal changes in the bone marrow (i.e. Modic changes, traumatic injuries with or without morphological modifications, but also other alterations related to degenerative spinal diseases).

The use of contrast media is limited to selected instances, i.e. to differentiate between degenerative, inflammatory and neoplastic diseases; in these instances the post contrast images must be

acquired using fat sat T1w sequences. On the conventional T1 images in fact the gadolinium uptake could hide lesion, whose signal, hypointense in basal conditions and increased by the contrast media, become not distinguishable from the natural high signal of the bone marrow, mainly represented by fat.

In the latest years the overall technical improvement of MRI system resulted in a notable increase in the spatial resolution of the diffusion weighted images (DWI), making them feasible for a more routinely use in the diagnostic of the cervical spine. Different DWI sequences have been developed in the different MRI system. As an example DWI demonstrate good accuracy in differentiating benign from malignant fractures and in diagnosing pyogenic collections.

Finally, it must be taken into account that MR imaging can directly demonstrate, with high sensitivity, the lesions of spinal cord, nerve roots and meningeal sheaths that are in some cases determined by degenerative changes of the osteo-discal structures.

Basic Findings in the Degenerative Disease of the Cervical Spine

The Disk

Disk degeneration starts early in life and frequently progresses relentlessly. The elderly frequently show disk degeneration of the cervical and lumbar tract.

The pathogenesis of intervertebral disk degeneration is unclear: multiple factors working separately (hereditary factors, age related vascular changes, vertebral endplate changes such as calcification), may lead to the impairment of the discal trophism. Mechanical factors as trauma, sports, or working related, may play a role.

Although the disk degeneration has to be considered a multi-factorial event, four are the elementary imaging features [12, 13] (Fig. 3.1):

- Loss of signal intensity of disk (MR imaging)
- Loss of height (all imaging modalities)
- Bulging (CT or MR imaging)
- Herniation (CT or MR imaging)

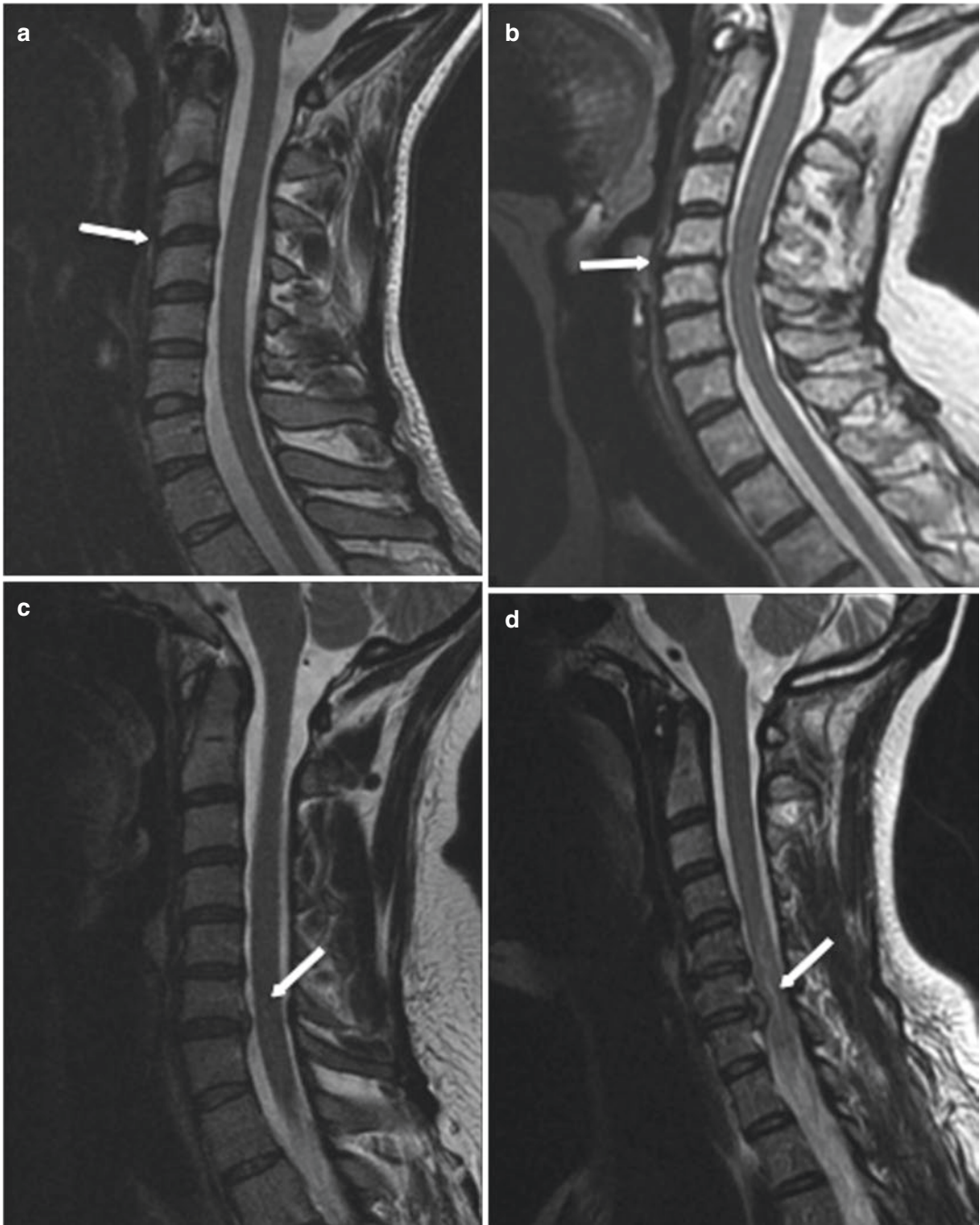


Fig. 3.1 Age-related disk modifications, disk bulging and disk herniation shown on sagittal FSE T2 images. Patient 1 (a): Minimal disk dehydration at C3–4 level (arrow), as demonstrated by low intensity signal on T2 images. Patient 2 (b): With the progression of degener-

ative changes, disk height is reduced and associated with mild spondylotic alteration at C4–5 level (arrow). Patient 3 (c): Posterior disk bulging at C6–7 level (arrow). Patient 4 (d): Disk herniation at C6–7 level (arrow)

The radial tear of the annulus that is often strictly associated with the other features, has to be considered the primary failure of the annulus itself [14]. The radial tear involves all layers on the annulus fibrosus and it is well described in MR imaging as high signal intensity tissue in the region of the disk, normally characterized by low signal intensity [15].

The disk degeneration processes evolve in a progressively loss of water, with a compromised integrity of the annulus fibrosus.

On MR imaging these signs are well evident on T2-w fast spin echo (FSE) or gradient echo (GRE) images with a loss of normal signal hyperintensity and an associated loss of height (often a vacuum phenomenon is demonstrated in CT or radiography). Frequently the disk degeneration is associated with an alteration of adjacent intervertebral body endplates (intervertebral osteochondrosis).

Modic [16] distinguishes three progressive grades of alteration adjacent to the endplates on MR imaging (Fig. 3.2), partially corresponding to the sclerosis described in radiographic or CT examination:

- Type I: hypointense on T1-w and hyperintense on T2-w bands which represent the marrow edema
- Type II: hyperintense T1-w and iso/hyperintense T2-w bands which represent the replacement by fatty marrow
- Type III: hypointense T1-w and T2-w bands which are characteristic of bone sclerosis.

The endplates bony marrow changes associated with degenerated disks needs to be however distinguished from other diseases, such as infection and metastases.

Spondilosis

Dehydration and fibrosis of the disk mean that static and dynamic mechanical stress can no longer spread through the horizontal plane of the disk, without altering it structurally. The disk

becomes the site of fissures, protrudes out and becomes thinner. Because of the displacement of disk material beyond the margins of the intervertebral disk space, a productive reaction is established, producing fibroblasts, in the adjacent vertebral margins: these phenomena represent the anatomic-pathological processes of spondylosis.

Osteophytes are the most characteristic sign of spondylosis and are more commonly found at levels C5–7; initially they are thin and have a horizontal course, then gradually enlarge until they weld in a “bridge” in the more advanced stages. Uncovertebral joints osteophytes characterize the framework of mono- or bilateral uncovertebral osteoarthritis: they grow into the vertebral foramina and can compress the spinal roots and extend into the intertransverse space, where they take relationship with the vertebral artery [17].

Interapophyseal joints osteophytes that protrude into the foramina will generally occupy the upper part and are rarely able to cause a radiculopathy by themselves. Instead they contribute to cause it in the presence of lateral herniated disk or severe uncovertebral osteoarthritis.

The development of anterior osteophytes in cervical spondylosis is usually modest and asymptomatic. Both radiography and CT can well demonstrate osteophytes. Even in the MR imaging, osteophytes can be studied with T2*-w sequences that well demonstrate bone structures, distinguishing from the adjacent degenerated disk.

Cervical spondylosis, both determined by age related degeneration or traumatic events, represents one of the most frequent causes of cervical instability and in late stages can determine non-specific symptoms (e.g. dysphagia), that may also mislead the clinical diagnosis. Therefore some studies tried to assess quantitative methods to evaluate and establish a grading of the spondylosis, basing on RX or CT examinations. Alizada et al. explored a radiographic index method based on evaluation of some features (cervical spine lordosis, the full flexion to full extension ROM, horizontal displacement, and cervical instability) on neutral and flexion-extension radiographs

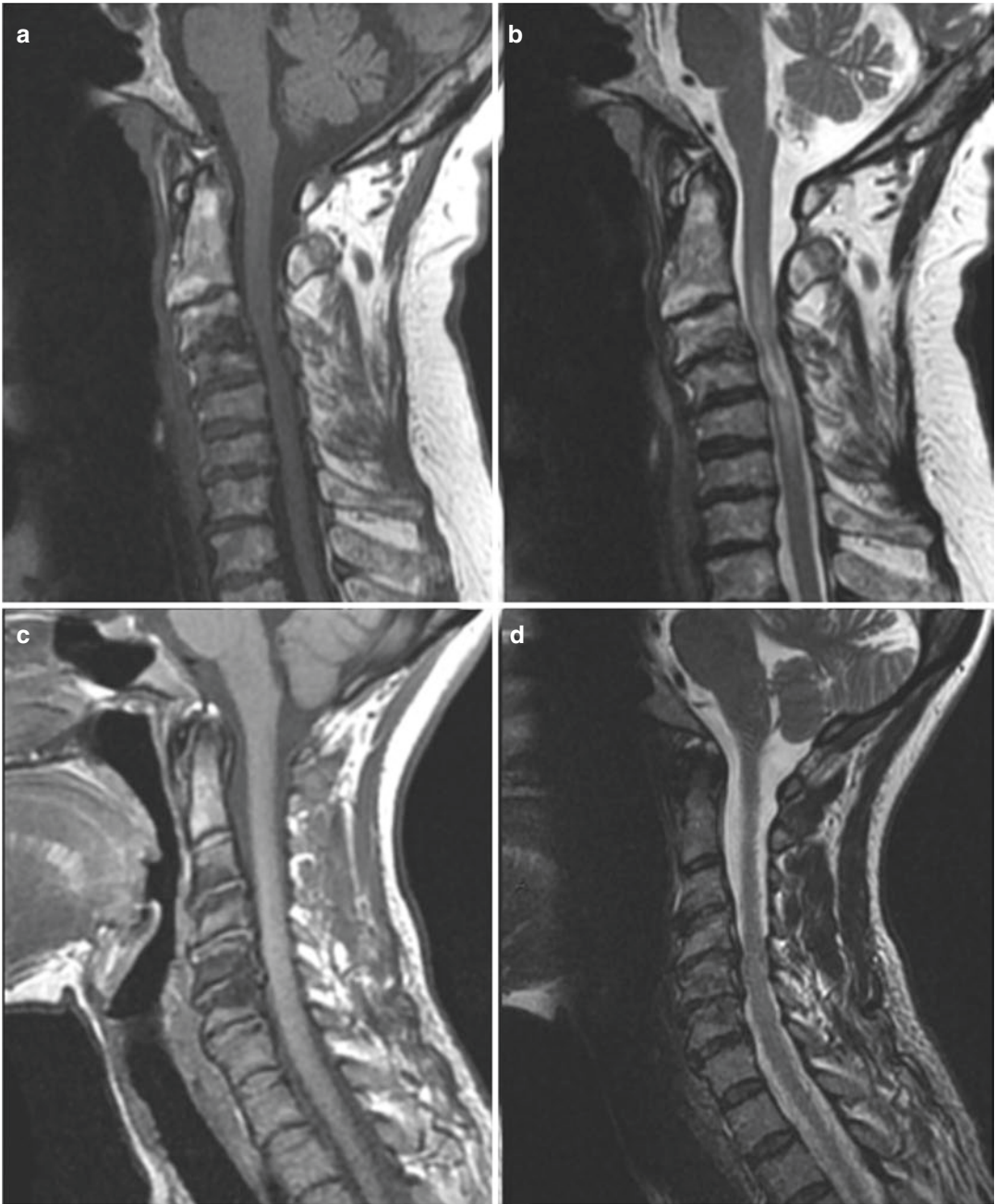


Fig. 3.2 Modic 2–3 alterations on sagittal FSE T1/T2 images. Patient 1: FSE sagittal T1 (a), FSE sagittal T2 (b). The vertebral endplates at C2–3 level show hyperintensity on both imaging sequences, due to fatty conversion of the normal bone marrow (Modic 2). Spondylosis results in

spondylotic myelopathy as demonstrated by central high signal of the compressed spinal cord. Patient 2: FSE sagittal T2 (c), FSE sagittal T2 (d). The vertebral endplates at C5–6 show hypointensity on both sequences, representing subchondral bony sclerosis (Modic 3)

[18]. Rydman et al tested a CT based score system evaluating both disc and facet joint degeneration in a population of adult patients with a history of trauma of cervical spine and symptoms of neck pain [19].

Cervical Facet Arthropathy

The degenerative facet disease or arthropathy has to be considered an osteoarthritis of sinovially lined apophyseal joints. Each apposing facet is composed of a thin uniform layer of dense cortical bone, and an overlying layer of cartilage. The facet joint is lined by synovium.

The degenerative process is not different from other synovial joints. It starts with hypertrophic degenerative inflammatory changes, followed by subluxation, that may produce gas (vacuum phenomenon). Lately there is a cartilage erosion with narrowed joint space. Mid and lower cervical spine represent the most common site.

Radiologically the early degenerative signs maybe difficult to demonstrate, while the later changes are well shown in radiography (facet arthrosis, vacuum phenomenon, mushroom caps facet appearance, sclerosis). Although CT with soft tissue window level well demonstrates the thickening and inflammatory changes of soft tissue, MR imaging obviously allows a much better visualization of the inflammatory changes and the facet effusion (linear T2-w images hyperintensity), but tends to overestimate, with the T2*-w images, the degree of foraminal and central canal narrowing. The gold standard about this topic should be represented by combination of fat-sat T2, standard T1 and post-contrast fat-sat T1w images (Fig. 3.3).

Ligament Degeneration

Cervical ligaments also undergo degenerative changes, represented by calcium deposits with the subsequent appearance of new bone forma-

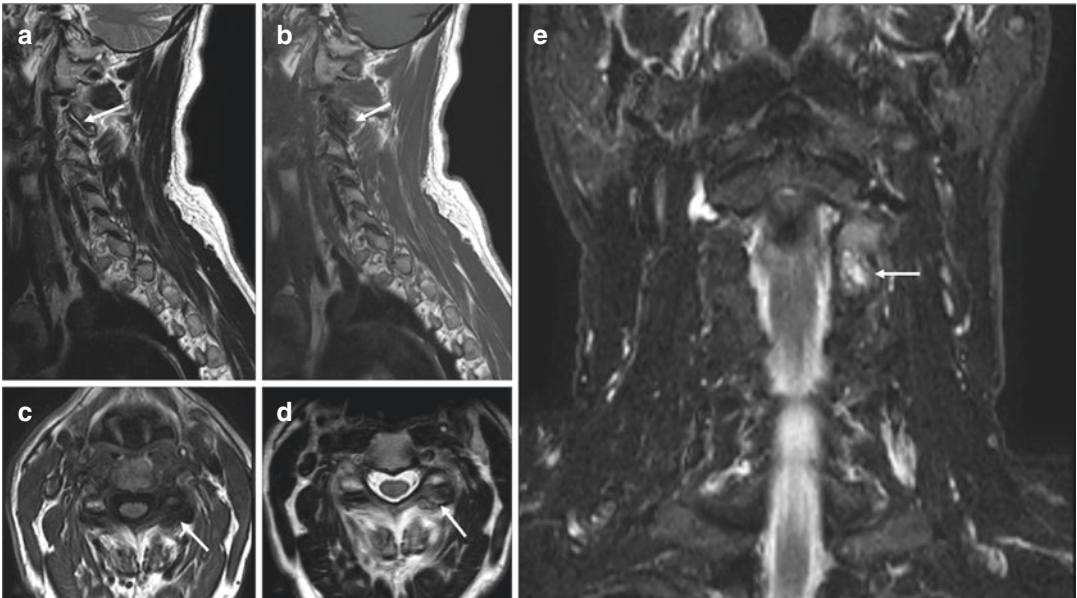


Fig 3.3 Cervical Facet Arthropathy. (a, b) Left parasagittal T2 (a) and T1 (b) w.i. (c, d) Axial T1 (c) and T2 (d) w.i. (e) Coronal T2 STIR. In this case of a Pt presenting with cervical pain on the left side at the level of the cranio-cervical junction the multiplanar T2w almost failed in demonstrating clear anomalies, showing only a minimal effusion in the C2–C3 lateral articular space [white arrow

in (a) and (c)]. The T1w better demonstrated a diffuse hypointensity of the medullar bone in the articular facets [white arrow in (b) and (d)]. The bony edema is finally evident on the coronal STIR images, both directly and in comparison with the hypointensity of the contralateral facets, due to the suppression of the fat signal, often high in the T2 FSE unsaturated slices [white arrow in (e)]

tion which compromise their firmness and elasticity. It should also be remembered that the involvement of disks and/or synovial joints is sufficient to induce ligamentous laxity, and consequently make alterations that entails the functional spinal unit (FSU). A FSU consists of two adjacent vertebrae, the intervertebral disk and all adjacent ligaments between them.

The calcified depositions and ossification are most frequently found both in the flaval and, especially, in the anterior and posterior longitudinal ligaments.

Degenerative Cervical Spine Instability

Stability can be defined as the ability of the vertebrae to maintain normal relations between them and to contain their mutual displacements, under the action of various postures and physiological loads. In normal conditions, the geometric characteristics of the vertebrae, a normal intradiscal pressure, the configuration of the facet joints and, above all, a correct ligament tension, are able to maintain correct motion between the FSU. When the above conditions are not preserved, the spine becomes unstable.

Despite the efforts of numerous authors to define the spinal instability, there is not a commonly shared definition; one of the biggest problems is represented by the fact that the concept has different meanings in various areas of clinical radiology and bioengineering. However, a reasonable definition has been proposed by White and Panjabi [20] that, supporting a bio-mechanical approach, define instability as a loss of “stiffness” of the motion segment in correspondence of which, under the action of a load, the motion determine abnormal displacement. In the biomechanical view, the “stiffness” is defined as the ratio between the loads applied to the structure and the resulting movement. The spine instability may therefore be the consequence of a trauma, of a degenerative disease and/or various other causes.

This premise is fundamental to allow an interpretation of cervical degenerative instability not

as a mere list of topographical radiological signs but as an alteration of the spinal disk-ligamentous complex as a whole. The various degenerative changes must be categorized in well-defined pathological successive phases according to Kirkaldy-Willis [21], which are:

- Phase of functional derangement
- Phase of instability
- Phase of fixity

Phase of Functional Derangement

Early degenerative changes (disk fissures and apophysis' synovitis) determine an inter-apophyseal joints stress that leads to a modest hypermobility of the vertebrae. Consequently, the hypermobility causes a repeated stress of nerve fibers with the onset of cervical acute pain. Facet joints subluxation can be associated with a disk herniation or a symptomatic synovitis.

At this phase the radiography is negative, so in the suspicion of a herniated disk it is necessary to acquire CT or MR imaging.

Phase of Instability

With the advance of functional derangement, degenerative phenomena worsen both on discosomatic complex (i.e. reduction of disk space, vacuum phenomenon, intervertebral osteochondrosis) and on zygapophyseal joints (sclerosis, “mushroom” deformation of articular pillars, articular effusion). Consequently radiculopathy or myelo-radiculopathy may emerge at this phase as a result of disk herniations; also a spondylolisthesis of the vertebra affected (degenerative spondylolisthesis) may result in dynamic narrowing of central canal and/or foraminal stenosis. The radiographic study, when made in LL projection, in flexion and extension (dynamic study), is able to detect not only the degree of listhesis but also to determine if it is fixed or unstable (Fig. 3.4).

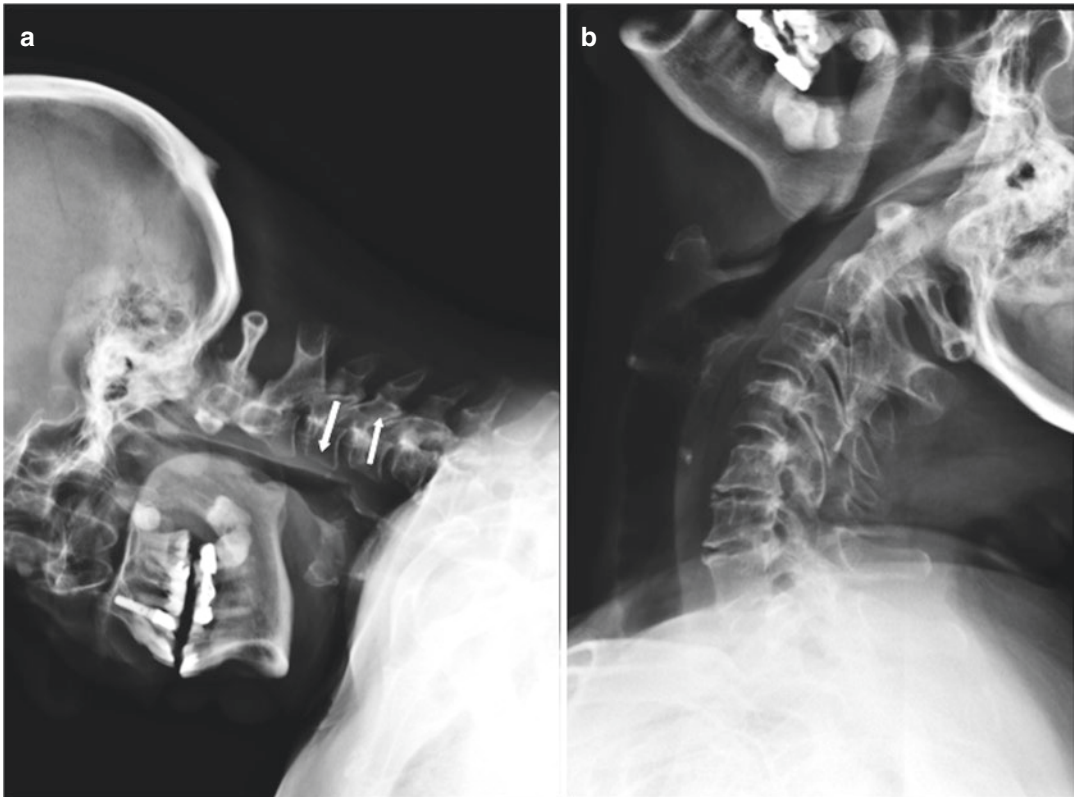


Fig. 3.4 Degenerative instability on flexion/extension radiography. Flexion (**a**) and extension (**b**). Minimal degenerative spondylolisthesis C3–4 evident on the flex-

ion radiogram (arrows, “phase of instability” according to Kirkaldy-Willis) with complete reduction on extension radiogram

Phase of Fixity

The findings are those of advanced osteoarthritis, with loss of motion, joint deformation and above all an increase in osteoproliferative phenomena (osteophytes and hypertrophy of the articular pillars); these alterations may lead to central canal stenosis. Conventional radiology is able to highlight osteoproliferative changes but not to assess their effects on neurovascular structures, and therefore they should be investigated with CT and MR imaging.

Cranio-Cervical Junction Degenerative Disease

The joint most frequently subject to degenerative changes in the craniocervical junction is the atlanto-odontoid. Atlantoaxial advanced degen-

erative changes are the main cause of the onset of symptoms (headache), with concomitant reduction in mobility. Also, it has been suggested that the onset of vertigo can be referred to a strict relation between upper cervical spine afferent fibers and vestibular and oculomotor nuclei [22].

Sometimes degenerative changes can lead to the formation of abundant inflammatory reactive tissue, mainly posterior to the odontoid process, that could determine an encroachment on the ventral surface of the spinal cord (inflammatory pseudotumor).

Imaging

CT and MR axial images, as in the subaxial cervical spine, provide a good evaluation of the spinal canal stenosis, which is often associated with

the degenerative changes in the crano-cervical junction; MR imaging is also capable to evaluate compression on the medulla oblongata and the subsequent onset of myelomalacia (characterized by hyperintensity on T2-w images). Moreover, the MR imaging can differentiate hypertrophic pseudotumoral changes of the CCJ (Fig. 3.5). Post-contrast images are useful to exclude/identify inflammatory changes (pannus).

Subaxial Cervical Spine Degenerative Disease

Cervical Disk Herniation

Terminology

The general term of “herniated disk” means the displacement of disk material beyond the margins of the intervertebral disk space and repre-

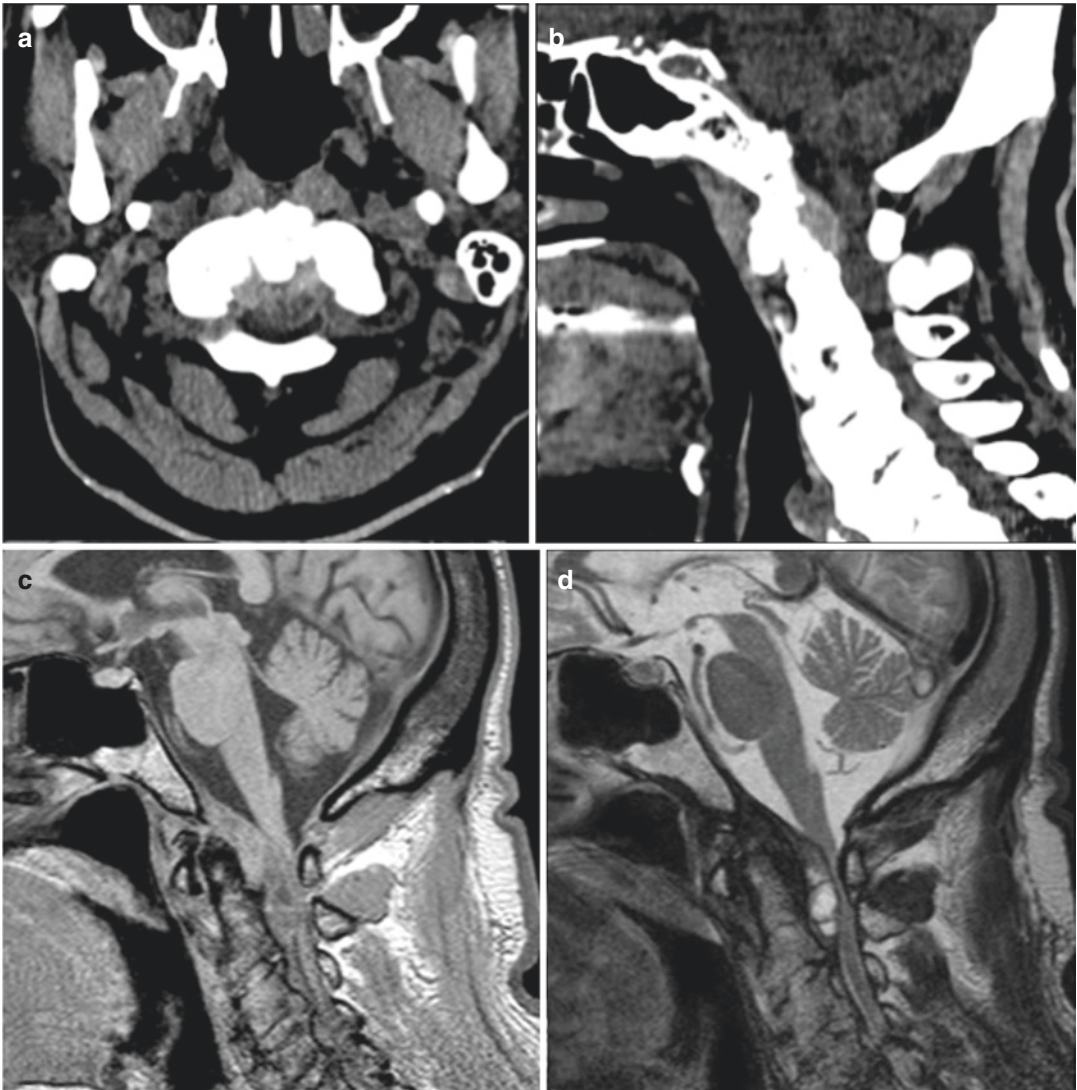


Fig. 3.5 Pseudotumor of the CCJ; CT and MR imaging. CT axial (a) and sagittal (b) images, sagittal GRE T1 (c) and FSE T2 (d) images. Abundant retro-odontoid inflam-

matory tissue at C0–C1 level, resulting in severe spinal cord compression

sents one of the major causes of neck pain. There are not universally accepted terminology and classification to define various pattern of disk herniation; different definitions are often used to describe the same type of hernia. A purely pathological classification of disk herniation is not suitable in daily radiological practice; i.e., the terms disk prolapse or disk herniation, respectively indicating that a portion of the nucleus pulposus has made its way through a fissure that involves only the innermost fibers of the annulus (prolapse), and the disk material that has gone through the whole annulus fibrosus, but not the posterior longitudinal ligament (disk herniation). However, since these two pathological conditions are not differentiable from each other even with MRI (both can manifest as focal contour deformities of disk), it is better not to make such a distinction. Morphologically we can distinguish protruded from extruded hernias: a disk protrusion is a herniated disk in which the distance between the edges of the disk herniation is less than the distance between the edges of the base; conversely, a disk extrusion is a herniated disk in which the distance between the edges of the disk material is greater than the distance at the base [23, 24].

Even if a universally accepted classification is not forthcoming yet, the differentiation between the “bulging disk” and the “hernia” is necessary in the clinical practice.

Bulging Disk (Fig. 3.6)

The “bulging disk” is characterized by wide/diffuse displacement of disk material beyond the normal limits of the intervertebral space, while the herniated disk is a focal dislocation. For wide/diffuse dislocation is meant a dislocation that affects more than 50% (180°) of the circumference of disk, while a dislocation is defined focal when interesting not more than 25% of the circumference of the disk. It is important to emphasize that the “bulging disk”, a common finding in people over the fourth decade, may be associated with reduction in disk height and does not necessarily represent a pathological condition.

In the presence of a bulging disk, the posterior dislocation of the disk tissue is typically symmetrical and maximum on the median line, but occasionally it is possible to observe also a focal disk displacement on one side or, even more rarely bilateral focal protrusions. In a relatively narrow spinal canal, the bulging disk can flatten the dural sac surface, but only rarely and in the

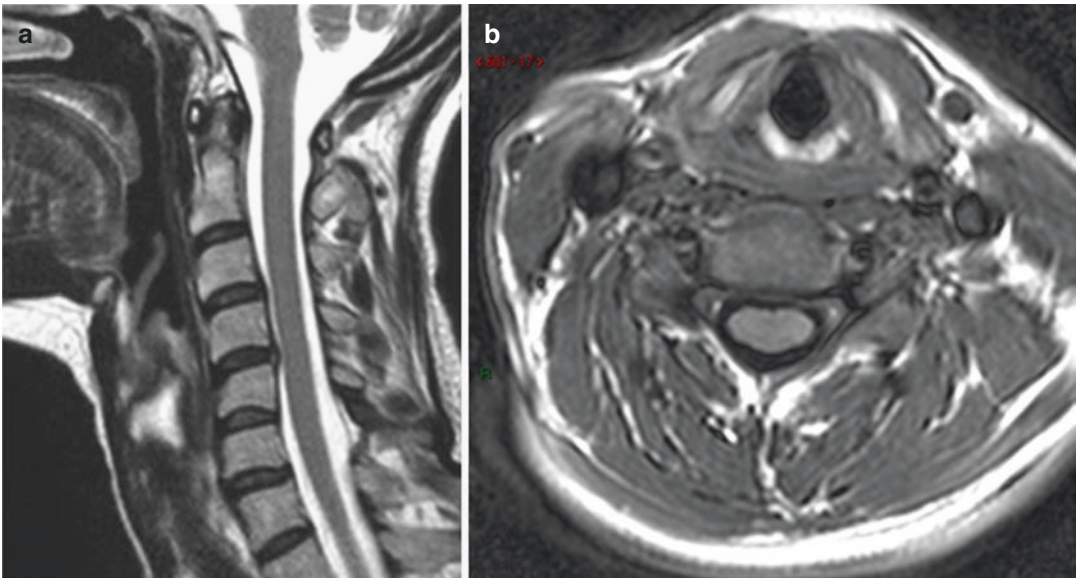


Fig. 3.6 Bulging disk. Sagittal FSE T2 (a) and axial FSE T1 (b) images. The C4–5 disk presents minimal diffuse bulging of its margins, with subtle effect on the ventral surface of the thecal sac

presence of a marked stenosis, it results in a true compression of the spinal cord or nerve roots.

Cervical Herniation: Subtypes

A herniated disk can occur in any direction, although those that have clinical relevance occupy the spinal canal or radicular canal and encroach the dural sac and/or nerve roots.

According to the location they are divided as follows (moving from central to lateral):

- “Central” hernia: extends into the spinal canal along the midline, compresses and deforms the epidural surface of the dural sac and sometimes, according to its size, is so voluminous that may cause a bilateral radiculopathy and/or myelopathy (Fig. 3.7);
- “Lateral/Paramedian” (Right/Left) hernia: not on the median line, but does not extend into the lateral recess. The herniated material displaces the epidural fat and may occupy the lateral recess, at the origin of the nerve root. It is responsible for a unilateral radiculopathy (Fig. 3.8);
- “Foraminal/extraforaminal” hernia: occupy the radicular (foraminal) canal, or extends beyond the corresponding foramen (forami-

nal/extraforaminal). Only the foraminal component has clinical relevance due to compression on the nerve root (Fig. 3.9).

By definition the herniated material, which can migrate upward or downward, is always in continuity with the intervertebral disk. The hernia can be more analytically described, in a MR study, as trans-ligamentous or sub-ligamentous, depending on the integrity of the posterior longitudinal ligament (PLL).

When a fragment of disk tissue is located in the central canal not in continuity with the disk, we use the term of free fragment. This fragment can migrate cranially or caudally and can thus impress a nerve root above or below the level from which it originated.

Although they may have, like all other disk herniations, an acute post-traumatic onset, are generally the result of degenerative processes of intervertebral disks such as the reduction in height of the intervertebral space and osteophytes that encroach the medulla or nerve roots. The evaluation of the relationship between herniated tissue and osteophytes is very important; in particular, we must distinguish between hernias where the disk component prevail (“soft hernia”)

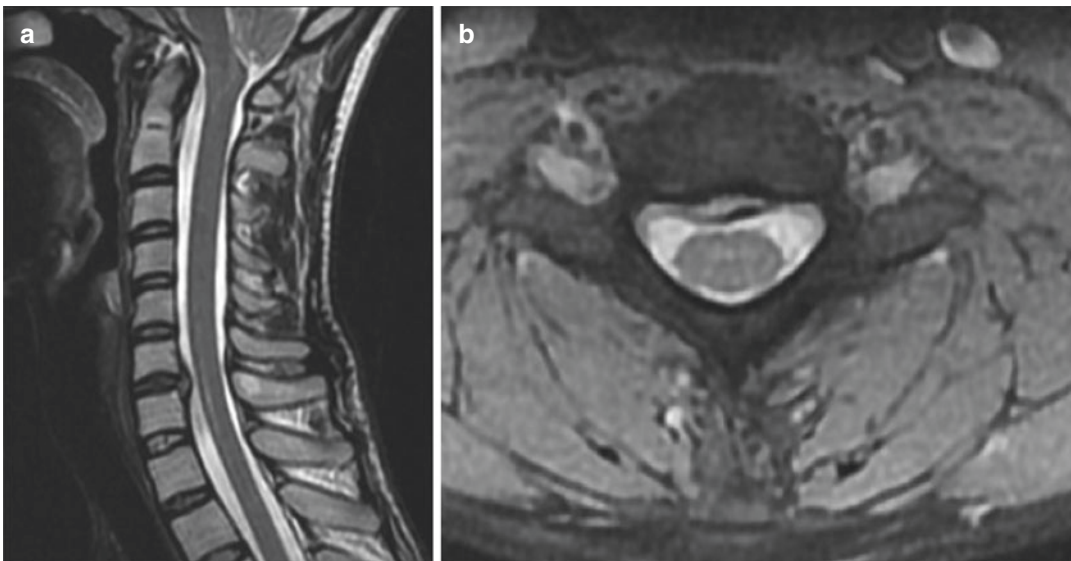


Fig. 3.7 Central disk herniation. Sagittal FSE T2 (a) and axial GRE T2 with fat suppression (b) images. It is evident a focal C6–7 protrusion/herniation of disk material deforming the ventral surface of the thecal sac on the midline

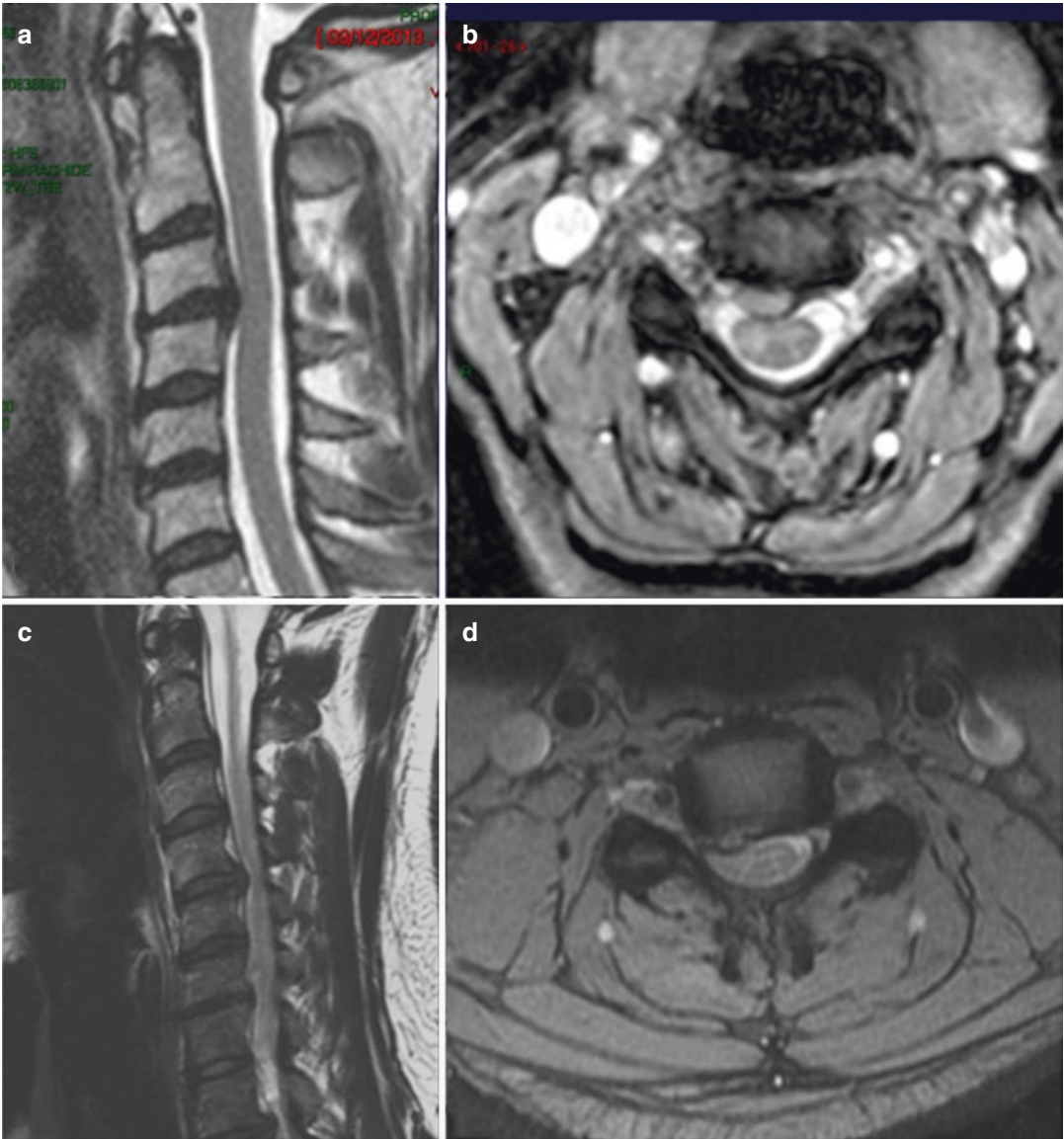


Fig. 3.8 Lateral disk herniations (posterior paramedian/posterolateral). Patient 1: Sagittal FSE T2 (a) and axial GRE T2 with fat suppression (b) images. The C3–4 paramedian disk herniation results in minimal impingement

on the right hemicord. Patient 2: Sagittal FSE T2 (c) and axial GRE T2 with fat suppression (d) images. The C4–5 posterolateral disk herniation occupies the right lateral recess with compression of the C5 nerve root

from those that are completely contained in a shell bone (“hard hernia”). In the latter, the surgical outcome is generally worse.

Cervical disk herniations are less frequent than lumbar because the cervical disks and vertebrae sustain less weight and the uncinete processes play an important role in containing the herniated material. The cervical hernia is more

common laterally, because in that location the posterior longitudinal ligament is less tough. Cervical herniations most commonly occur at the C5–6 and C6–7 levels.

Cervical Herniation: Imaging

The peculiar anatomy of cervical spine, where intervertebral disks are thinner, radicular canals

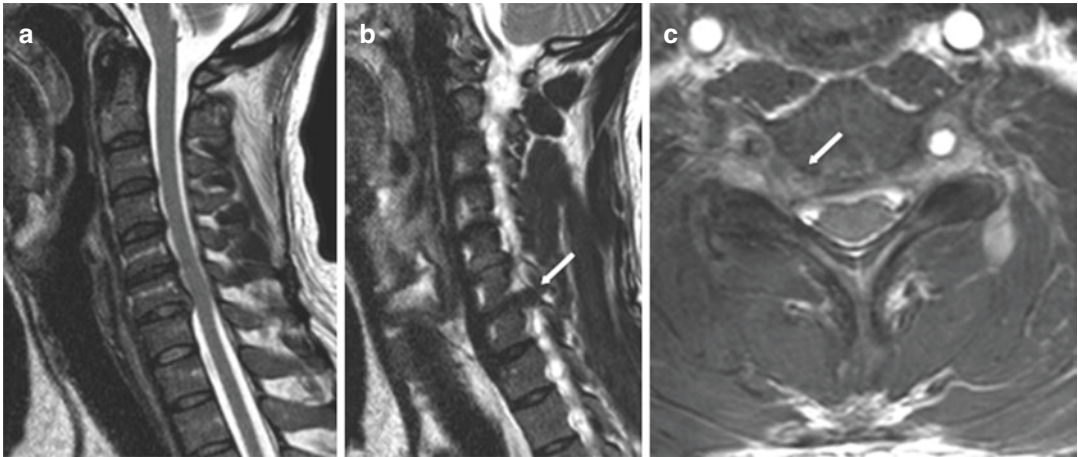


Fig. 3.9 Foraminal C6–7 disk herniation. Sagittal FSE T2 on the midline (a), right parasagittal FSE T2 (b) and axial FSE T2 (c). On the midline there is only minimal

disk bulging while the large disk herniation [arrow in (b) and (c)] completely occupies the right neuroforamen

and foramina are shorter and there is much less epidural fat, should always be taken into account while executing a CT scan. CT is typically used to detect the different hernia components (“soft” from “hard” hernias) and in the evaluation of bony structures. The multiplanar oblique reconstructions perpendicular to the major axis of the radicular canals provide, for example, an excellent assessment of the size of the foramina and their possible stenosis due to the presence of uncovertebral osteophytes.

The detection of a small disk herniation may however be difficult for the scarce representation of epidural fat or, in patients with short and thick neck, for the superposition of the shoulders and the rib cage. The use of intravenous contrast medium can evidenciate the conspicuity of disk herniation thanks to the enhancement of epidural veins and of the associated granulation tissue. Although CT maybe useful in the diagnosis of cervical hernia, post-contrast examination are usually not required to make the diagnosis because of the clearcut superiority of MRI. Before scheduling a surgical procedure, however, it may be very important to evaluate the status of the bony walls of the central spinal canal and radicular canal, as shown by CT. In fact, disk herniation is often a contributing cause of the symptoms and may be associated, for example, to the stenosis of

a radicular canal secondary to uncovertebral osteophytes, which are better visualized on CT.

MRI is definitely the examination of choice in patients with signs of radiculopathy or myelopathy caused by disk herniations. The MRI study should be executed using sagittal and axial SE T1-w images, the corresponding FSE T2-w images, and 2D/3D GRE T2*-w at the levels where there is a suspicion of disk disease. T1-w images provide detailed anatomical information; the disk appears hypointense, similar to the ligamentous structures and osteophytes. Because the cerebrospinal fluid (CSF) also presents low signal intensity and the epidural fat is scarcely evident, there is little contrast between extradural structures and CSF. It is therefore difficult, in axial T1-w images, to differentiate a small amount of herniated tissue from an osteophyte. Small herniated cervical disks are certainly easier to detect in 2D/3D T2*-w images, in which the bone is more hypointense, fluids are very hyperintense and therefore it is easier to differentiate the herniated disk from the bone and the adjacent osteophytes. Migrated fragments can sometimes mimics osteophytes, because of their low signal intensity, and are better visualized on GRE T2*-w images than on FSE T2-w images. The thinning and low signal of PLL on GRE T2*-w is characteristic of acute disk herniation [25] (Fig. 3.10).

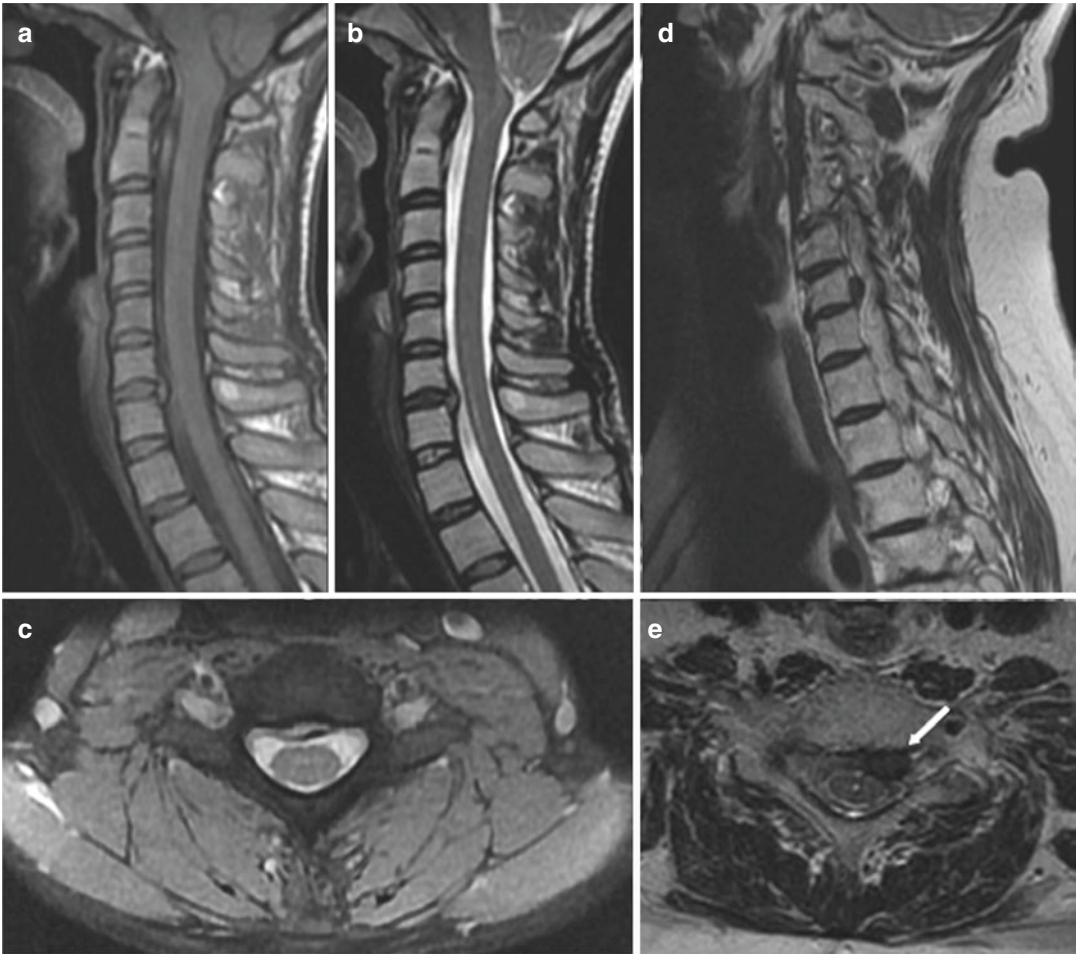


Fig. 3.10 Disk herniations, MR imaging. Patient 1: sagittal FSE T1 (a), sagittal FSE T2 (b), axial GRE T2 (c). Acute disk herniation with high signal intensity at C6–7

level. Patient 2: sagittal FSE T2 (d), axial FSE T2 (e). Lateral disk herniation with cranially migrated disk fragment [arrow in (e)] which shows low signal on T2 images

Stenosis

Central canal stenosis define the narrowing of the vertebral canal and/or lateral recesses and radicular canal, which can lead to compression of the nerve roots or spinal cord.

Patients with cervical stenosis have insidious symptoms onset, expression of mono or bilateral radiculopathy or myelopathy (e.g., upper limb paraparesis or dysesthesia).

The neck pain is often associated, but is not specific. Early diagnosis is essential, since there is no spontaneous regression of the process and

the surgery prevents the progression of the symptoms and of the spinal cord damage.

Using etiological criteria it is possible to distinguish:

- Congenital stenosis (idiopathic, dysplasia, achondroplasia, mucopolysaccharidosis): characterized by short and stubby peduncles, shortness of the interpeduncular and sagittal diameter and hypertrophy and verticalization of the laminae; the central canal appears narrowed, as well as reduced, or completely absent, appears the epidural fat;

- Acquired stenosis: can be the result of surgery, traumatic lesions or neoplastic but, more frequently, derive from degenerative alterations of vertebral bodies (osteophytes), of articular pillars (hypertrophic degenerative osteophytes, subluxation), intervertebral disks (“bulging”, herniated disk), of flaval ligament (hyperplasia, calcification) and/or of posterior longitudinal ligament ossification. The same reduction in height of the intervertebral space, due to disk degeneration, can determine the shortening and thickening of the intervertebral ligaments, resulting in the encroachment on the dural sac;
- Mixed stenosis: are the most frequent in clinical practice and derive from the overlap of an acquired form on a condition of congenital stenosis; in this case, a disk protrusion and/or osteophytosis, even modest, may lead to severe nerve root or spinal cord compression.

Using topographic criteria, stenosis may be divided into:

- Central: characterized by a reduction in the size of the central canal, that in degenerative forms is supported by the “bulging” disk, hyperplasia and/or calcification of the flaval ligaments, osteophytes and degenerative articular pillars hypertrophy.
- Lateral: include lateral recesses and foraminal stenosis. Lateral recesses stenosis is due to uncinat process hypertrophy, degenerative enlargement of a superior articular facet and/or osteophytosis. Foraminal stenosis is mostly supported by congenital factors (shortness of peduncles), by degenerative pathology of the disk (“bulging”) and posterolateral vertebral bodies osteophytosis.

Furthermore, measurement of the diameters of the canal is not very reliable, given the considerable individual variability. It is true, however, that at the cervical level there are two semeiological radiographic references that allow assessing the sagittal diameter of the central canal: the first coincides with the ideal line drawn along the posterior wall of the vertebral bodies; the second is

the spinolaminar line. This imaginary line joins the convergence points of the laminae of each vertebral body on the midline. Normally, the spinolaminar line is convex forward and is at least 3–4 mm away from the posterior edge of the articular pillars. If the spinolaminar line is overlapped to the zygapophyseal joints, it is possible to infer that the sagittal diameter of the cervical central canal is reduced.

Another method to assess spinal stenosis is the central canal-to-vertebral body ratio, also called “Torg-Pavlov ratio”. This is a ratio of the diameter of cervical canal to the width of cervical body. Less than 0.8 on radiography is consistent with cervical stenosis [26]. However, we can consider stenotic a cervical spinal canal with a width less than 13 mm [27]. CT better visualizes the causes of degenerative spinal stenosis, since it well demonstrates vertebral body and facet joints osteoproliferative processes, degenerative changes of intervertebral disks and calcification of flaval ligaments.

In case of degenerative spondylolisthesis, CT easily identifies subluxation of the zygapophyseal joints, the sign of “double arch” and, in the sagittal multiplanar reconstructions, dural sac impingement. CT also allows easier measurement of the diameter of the central canal, but it is not able to demonstrate the effects of the degenerative injury on the spinal cord. Moreover, in the cervical spine, the low amount of epidural fat and the relatively small size of the spinal canal is insufficient to assess a possible ligamentous hypertrophy.

Imaging

Good quality X-ray studies demonstrate the degenerative changes but not their compressive phenomena on the spinal cord, their extension (on sagittal images) and, above all, the direct effect on the nervous structures (edema, gliosis and myelomalacia). Because of these advantages, especially in the cervical spine, MR imaging represents the preferred imaging modality (Fig. 3.11). The root compression in the foramina is shown, in the sagittal T1-w images, by the dislocation or disappearing of periradicular fat; compression of the dural sac and disk degenera-

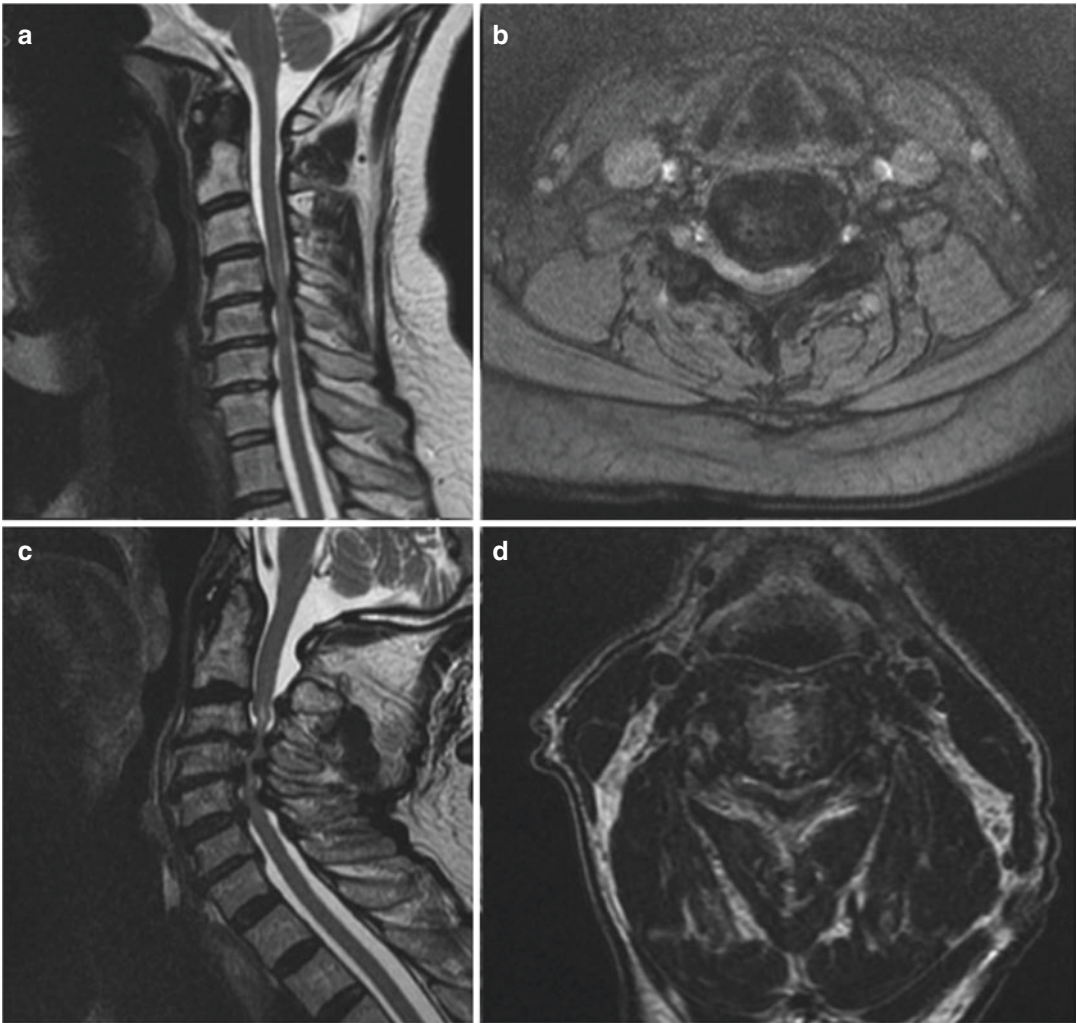


Fig. 3.11 Stenosis of the spinal canal, MR imaging. Patient 1: sagittal FSE T2 (a), axial GRE T2 (b). Posterior disk herniation associated to mild spondylosis at levels C4–5, C5–6 and C6–7 determine spinal canal stenosis with encroaching the spinal cord that presents intrinsic signal modifications. On axial images the degree of stenosis

is better evaluated. Patient 2: sagittal FSE T2 (c), axial FSE T2 (d). Advanced stages of spondylosis and disk degeneration/herniation. The central canal is almost completely obstructed. Spinal cord is severely compressed with reduction of its sagittal diameter and intrinsic signal modifications

tion, however, are more evident in the T2-w images. Using volume 3D GRE techniques with thin sections (1 mm or less) it is possible to obtain the best evaluation of cervical neural foramina [28]. Although CT can be used to detect narrowed neural foramina, the MR imaging using axial GRE T2*-w or post-contrast MR scans usually offers better results. The T2*-w images allow identification of osteophytes and differentiate them from adjacent disk herniation. Furthermore, it clearly demonstrates the ossification of the pos-

terior longitudinal ligaments and the flaval ligaments hypertrophy, due to the intrinsic high contrast that exists between these structures and the adjacent subarachnoid space. If the spinal cord is compressed from a long period, irreversible changes occur, namely myelomalacia and gliosis, with focal areas of high intensity signal in the cord on T2-w images [29], resulting in a more obvious reduction of the sagittal diameter of the spinal cord (atrophy) with increased evidence of the ventral fissure.

Specific Degenerative Diseases

Rheumatoid Arthritis

Even if Rheumatoid Arthritis is not a pure degenerative disease, we included this pathological entity in the chapter, because of the primary involvement of the cervical spine and the resemblance of its manifestations with those of the other degenerative diseases.

Rheumatoid arthritis (RA) is a chronic autoimmune disease that involves the small synovial joints leading to progressive destruction, with associated systemic involvement. The prevalence is 1% in general population, with female predilection (F:M 3:1), however males have a greater risk of developing advanced cervical involvement. The joint involvement in RA is symmetrical in the appendicular skeleton, while the axial skeleton is usually spared except for the cervical spine. The cervical spine is involved in up to 86% of patients and overall, RA is the most common inflammatory disorder that involves this rachidial segment. The synovial joints involved are the atlantooccipital and atlantoaxial joints. The progressive destruction of these joints leads to development of atlantoaxial instability (AAI) or forms of luxation or subluxation, in particular, atlanto-

axial subluxation (AAS), vertical axis subluxation (VS) or cranial settling, and subaxial subluxation (SAS). The entity of cervical spine involvement is related to multiple factors (duration of AR, severity of peripheral arthritis, duration of corticosteroids therapy, presence of rheumatoid nodules, serum values of RF).

The pathologic *primum movens* is the synovial membrane inflammation, sustained by a cascade of events, with influx of immune cells, including neutrophils, mast cells, and macrophages into the synovium, and local release of proinflammatory cytokines and small-molecule mediators of inflammation. The inflammation of the atlantoaxial joint (Fig. 3.12), facet joints, uncovertebral joints, retrodental bursa, interspinous ligament and ligaments around the atlas leads to the formation of a periodontium inflammatory pannus with progressive articular cartilage loss, formation of bony erosions and ligamentous destruction. Then follow cervical instability with ipermotility, while the successive step is the establishment of subluxations (atloaxial or subaxial) with consequent mechanical derangement of the segment (Fig. 3.13). The final consequences are the various compressive neurological and vascular manifestations.

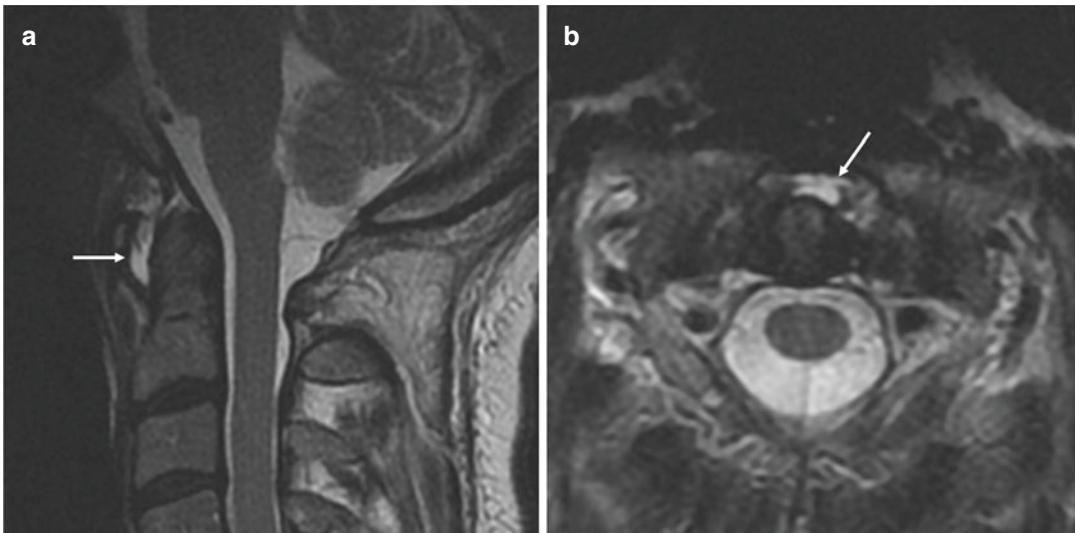


Fig. 3.12 Rheumatoid Arthritis, MR imaging. Sagittal FSE T2 (a) and Axial FSE T2 (b). Anterior subluxation, with presence of fluid and inflammatory tissue around the

dens (in particular anteriorly), with high signal in T2 sequences [white arrow in (a) (b)]. No signs of erosions in this case

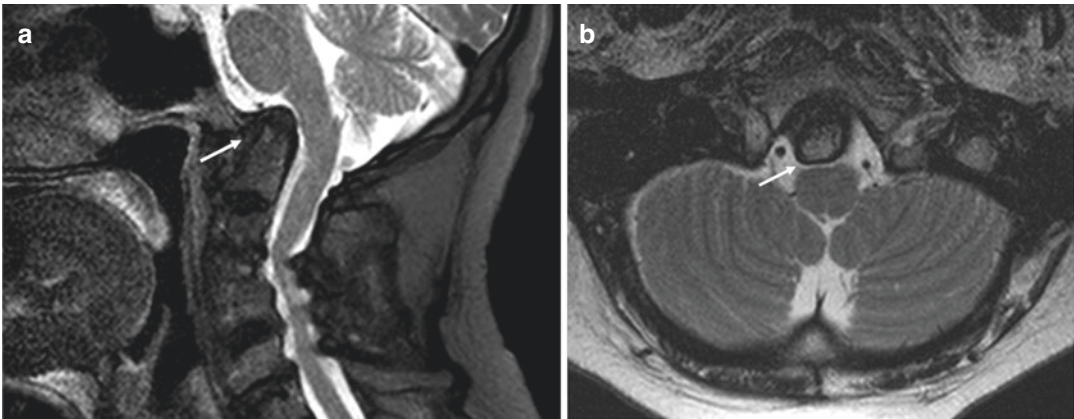


Fig. 3.13 Impressio basilaris in a Patient with rheumatoid arthritis, MR imaging. Sagittal FSE T2 (a) and Axial FSE T2 (b). (a) Vertical atlanto-axial luxation; the apex of dens lies above the foramen magnum (white arrow); in (b)

(white arrow) mild compression on the ventral surface of medulla oblongata is evident, without white matter involvement

The majority of patients with cervical involvement are asymptomatic at the moment of diagnosis. When symptomatic, the most common findings is neck pain, but there are multiple possible clinical presentations due to compression of cervical structures (cervical or cranial nerves, brainstem, spinal cord or vessels), or to cervical instability. Relatively common finding in symptomatic patients are different forms of pain, such as occipital headache (in case of cranial settling or AAI, due to compression of occipital nerves passing between the atlas and axis), migraines or neck, mastoid, ear, or facial pain (determined by the compression of the C2 spinal nerve or greater auricular nerve). The symptoms related to compression of the brainstem and/or vertebral arteries include tinnitus, vertigo, dysphagia, visual disturbance and diplopia. The symptoms related to cranial nerve compression are extremely variable: the most common are dysphagia (due to compression of the X or XI cranial nerves), dysarthria (due to the compression of the XII CN) and paresthesia, hypoesthesia or facial pain (due to compression of the nucleus of the spinal trigeminal tract). The myelopathy symptoms (with variable combination of muscle atrophy, weakness, gait impairment, dexterity impairment, limb paresthesias, hyperreflexia, spasticity, loss of proprioception, bowel or bladder disturbance), that

in the severe cases can lead to paralysis due to secondary syringomyelia, locked-in syndrome, or sudden death are related to the spinal cord compression. In physical examination Lhermitte's sign is reported in case of compression of the superior spinal cord and cervico-medullary junction. Cervical instability, in particular AAI, is related to sensation of the head falling forward upon flexion. Moreover, if the consequences of cervical instability determine kinking of the vertebral arteries, there is an increased risk of vertebrobasilar thromboembolism.

Pharmacologic therapy of RA is based on administration of glucocorticoids (GC), disease-modifying antirheumatic drugs (DMARD), and or biologic agents (BA). DMARDs and BAs decrease the incidence of cervical spinal involvement, but they are not effective in attenuating the progressive destructive disease course in the cervical spine when already present. This consideration highlights the necessity of an early diagnosis and treatment of cervical spine involvement in RA.

Imaging

Plain radiograph is usually the first examination, particularly in asymptomatic patients. The standard examination should include plain radiographs with dynamic flexion-extension and open

mouth views for odontoid. These projections are reliable in determining bone alignment and deformities. However, the assessment of instability of cervical spine based on plain films may vary. Moreover, some imaging features are not completely analyzable in plain radiographs, in particular bony erosions, the status of cranio-cervical junction and cervicothoracic junction and the characteristics of inflammatory pannus and spinal cord compression. In case of plain radiographs findings that confirm or pose a suspect for RA, or in case of symptoms (neck pain, neurological symptoms), computed tomography (CT) or magnetic resonance imaging (MRI) are indicated. CT scan with multiplanar reconstruction best depicts bony erosions and the presence of ankylosis or pseudarthrosis, and may be used in surgical planning. MRI has a specific indication on all patients with myelopathy or radiculopathy, because represent the best imaging modality for soft tissue and spinal cord assessment. The possibility to acquire dynamic flexion-extension MRI sequences is useful to diagnose subarachnoid encroachment that cannot be ruled out in static MRI.

Diffuse Idiopathic Skeletal Hyperostosis Syndrome

The Diffuse Idiopathic Skeletal Hyperostosis or DISH, (also known as Forestier disease, senile ankylosing hyperostosis and asymmetrical skeletal hyperostosis) is a not uncommon degenerative disorder in the elderly population, with a reported prevalence in some study of 10% in patients over 70 years [30, 31]. It is characterized by excessive ossification along the anterior longitudinal ligament of the spine, resulting in bridging osteophytes. In the 1970s, Resnick established specific radiological criteria for the diagnosis of DISH [32]: (1) presence of flowing calcification and ossification along the anterolateral aspect of at least four contiguous vertebral bodies; (2) relative preservation of intervertebral disk height in the involved vertebral segments without degenerative disk disease; (3) absence of apophyseal joints ankylosis and sacroiliac joint erosion, scler-

osis or bony fusion [33]. Extra-spinal ossification in DISH may occur at the ligamentous attachments and para-articular soft tissues.

DISH is largely asymptomatic and it is usually incidentally detected. The exact etiology of the syndrome is unknown: the DISH could be considered an expression of the ossificans diathesis, typical of the advanced age, that leads to the production of bone tissue at the insertions of tendons and ligaments on the skeletal structures (entheses), to ligaments calcification and ossification, and finally to the formation of para-articular osteophytes [1]. The spine is the elective target of the disease, pointing out that other skeletal regions may also be involved.

The prevalence is highly variable (2.9–42.0%) and depends on different factors: the demographic background, the used diagnostic criteria and the presence of concomitant risk factors, such as older age, metabolic factors (hypertension, obesity, diabetes mellitus), and cardiovascular diseases [34].

Imaging

The radiological findings results directly from the histopathologic alterations of the spine. A characteristic aspect of the DISH is that the ossification of the ALL is more pronounced at the level of the disk spaces, creating a “bulky” aspect of the ventral spine profile.

In the first stages of the disease, radiography may show a fine ossification (with thickness of 2 mm or less); with the progression of the illness it is possible to observe the development of large syndesmophytes (a syndesmophyte is defined as a bony growth originating within a ligament). The typical site of syndesmophytes formation is the anterior aspects of vertebral body (because of the involvement of ALL).

Radiography is inadequate for evaluating the extent of the compression caused by the large syndesmophytes on trachea, bronchi, or esophagus. In this case, a CT study of the spine, with multiplanar reconstruction, would be helpful (Fig. 3.14).

CT play also a role in the evaluation of complications, such as fracture, spinal canal stenosis secondary to associated ossification of the poste-



Fig. 3.14 Diffuse Idiopathic Skeletal Hyperostosis Syndrome (DISH), radiography and CT. Lateral radiogram in standing position (a) and CT sagittal images (b). Diffuse ossification along the ALL with bridging osteo-

phytes from C2 to C7 is well evident, with preserved disk height. The findings are well demonstrated on CT examination, with a better visualization of the disease extension

rior longitudinal ligament, and pressure effects on the hypopharynx. The only indication for the MRI is to show/rule out cord compression when DISH is associated with an ossified PLL, as it is observed in a minority of patients [35].

The criteria most frequently employed to establish a diagnosis of DISH are those described by Resnick and Niwayama (bridging of four adjacent vertebral bodies by new formed bone, without severe loss of the intervertebral disc height and without degeneration of the apophyseal and sacroiliac joints probably reflecting findings related to the end stage of the disease [33]. Kuperus et al proposed the CT parameters to distinguish between no DISH, early DISH, and definite DISH in order to consider diagnostic criteria to establish the diagnosis in the early stage. The evaluated features were the presence and location of bone bridges, the degree of flow of the new formed bone and the location of new bone formation, giving points to each characteristic, thus realizing a score system [36].

Ossification of the Posterior Longitudinal Ligament

Ossification of the posterior longitudinal ligament (OPLL) is a spine disorder that usually affects individuals between the fifth and seventh decade of life, more frequently males; a higher incidence in the Japanese population has been reported [37]. The disease commonly involves the cervical regions of the spine and is clinically characterized by myeloradiculopathy, even if the OPLL may be often asymptomatic.

It has been proposed that pathogenesis of OPLL may be related to disk herniation and/or to a diffuse hyperostotic process [38].

OPLL can have a progressive course both in patient that underwent decompressive posterior surgery and in asymptomatic, not-surgically treated patients. Some studies focused on findings those risk factors. Lee et al found a greater risk for post-operative OPLL progression in patients that underwent posterior laminoplasty

for specific type of disc involvement and in case of increased range of motion (ROM) evaluated on dynamic plain radiographs; increased ROM is also a risk factor for development of cervical myelopathy [39]. Doi et al investigated the risk factors for OPLL progression in asymptomatic patients, finding that younger age, OPLL involvement of multiple vertebral levels, continuous type of OPLL and higher serum levels of uric acid represent higher risk of progression in this subset of patients [40].

Imaging

On plain radiography a continuous calcification along the posterior longitudinal ligament is observed, especially on the intermediate tract of the cervical spine (C3–5); the associated disk

degeneration and facet ankylosis are often minimal.

CT has a higher sensitivity in the assessment of the calcification extension; in some cases the axial images can show specific patterns of calcification of the ligament (“upside-down T” and “bowtie”). MR imaging shows the spinal cord lesion that can be associated, particularly in those cases in which the ossification thickness is greater (Fig. 3.15).

In some patients with OPLL it is possible to detect an extensive calcification of the ALL or other signs of DISH; when it happens, differential diagnosis with inflammatory arthropathy is made possible by observing the absence of facet joint ankylosis and scarcity of associated disk degeneration [37].

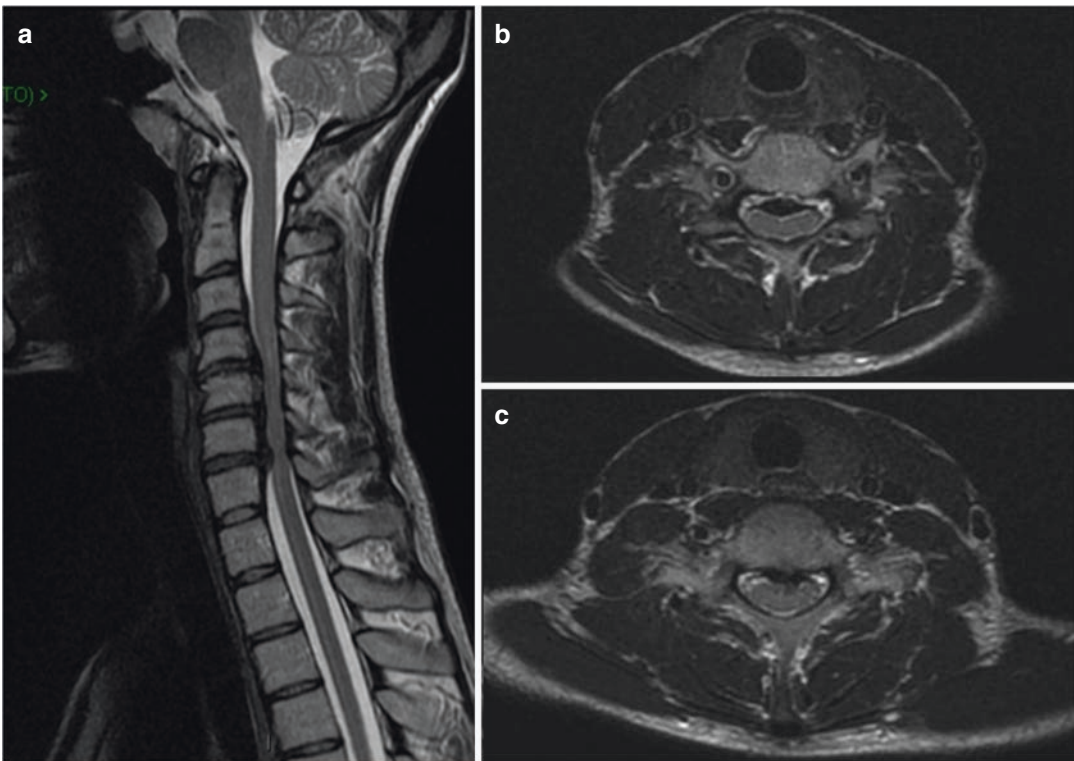


Fig. 3.15 Ossification of Posterior Longitudinal Ligament (OPLL), MR imaging. Sagittal FSE T2 (a) and axial FSE T2 (b, c). Ossification of the posterior longitudinal ligament is located at C3–C6 levels, in the interme-

diante tract of the cervical spine. The spinal cord shows mild hypertensity at that level (edema/gliosis) due to compression from the thickened ligament

Destructive Spondyloarthropathy of the Cervical Spine in Long-Term Hemodialyzed Patients

Destructive Spondyloarthropathy (DSA) is characterized on plain radiography by a notable reduction of the intervertebral disk space associated with erosions and cysts of the adjacent endplates and minimal osteophytosis. Typically, multiple vertebral bodies are involved: the lower part of the cervical spine (C5–7) is most frequently affected, though the CCJ may also be involved. Clinically, DSA can lead to medullary compression, which requires surgical decompression and stabilization. However, neurological symptoms are rare. The prevalence of DSA is difficult to establish: it varies from 5 to 25.3% in long-term hemodialyzed patients [41].

The exact pathogenesis of DSA is not well understood: it could be the direct consequence of the hemodialysis-related systemic amyloidosis. There are many risk factors associated with the onset of the DSA, such as the duration of renal failure, the age of onset, the duration of hemodialysis, dialysis membranes and the basic clinical condition of the patient, but to date the natural history of this syndrome is unclear and no effective treatments are available.

In a study of Nagamachi et al has been reported that the age at the onset of hemodialysis is also related with the progression of destructive changes, differently from the duration of hemodialysis that did not show such correlation [42].

Imaging

The radiographic signs of the syndrome include a severe reduction of the intervertebral disk space associated with erosions and/or cysts of the adjacent endplates, and minimal osteophytes formation.

On radiography, in the early stages of the DSA it is also possible to detect signs of enthesopathy, mimicking an early ankylosing spondylitis. As the pathology progresses, endplate destruction associated with a soft tissue mass is established, very similar to the spondylodiscitis appearance. These alterations lead to vertebral body collapse, spondylolisthesis or spondylolysis.

The degenerative process, with pseudotumors and bone erosions, can sometimes involve the CCJ, although it is uncommon. A relevant clinical problem is to rule out infections in symptomatic hemodialyzed patients (who present an increased risk of infective diseases) with destructive vertebral lesions. The radiologist should be able to distinguish DSA from spondylodiscitis; if the disks show low signal on T2-w and STIR (Short Tau Inversion Recovery) images, DSA is more likely.

Ossification of Flaval Ligaments

It is a degenerative disorder characterized by the ossification of flaval ligaments. The pathogenesis is unclear and probably associated with metabolic disorders (with hydroxyapatite or calcium pyro-phosphate deposition in ligaments).

Ossification of flaval ligaments appears as a linear thickening of flaval ligament similar to adjacent vertebral marrow ossification. The ossification is typically symmetric and bilateral; it is often diagnosed incidentally during imaging study ordered for other reasons.

Imaging

On radiography, when appreciable, ossification of flaval ligaments appears as a thin calcification located anteriorly to laminae.

CT is the best imaging modality to show ossification, but it is inadequate in order to determine the possible spinal cord involvement. On CT, ossification of flaval ligaments appears as a hyperdense thickening within the ligament, best shown on axial native scans with the characteristic V-shaped image.

MR imaging may easily detect not only ossification of the ligaments but also the secondary effect on the spinal cord. On T1-w images the ossification of flaval ligaments appears as a hypointense (thinner lesions) to hyperintense (thicker lesions) linear mass within the ligaments. On T2-w images, it appears as a linear hypointensity associated or not with myelomalacia, due to cord compression. On GRE T2*-w images, the flaval ligaments appear as a thickened hypointense

band, and it is difficult to estimate the actual degree of canal narrowing due to susceptibility artefact [6].

Calcium Pyrophosphate Deposition Disease

Calcium pyrophosphate deposition disease (CPPD) is a metabolic arthropathy, also known as pseudogout, caused by a proliferation and deposition of calcium pyrophosphate dihydrate in and around the joints, especially in articular cartilage and fibrocartilage, with possible involvement of CCJ, namely the peri-odontoid structures. It is characterized by linear disk or ligament calcific deposits. The exact etiology of the syndrome is unclear; it may be associated with hyperparathyroidism, hemochromatosis, gout or hypophosphatasia.

Imaging

Radiography may demonstrate linear calcifications within the disk, and it is often associated with calcification of the pubic symphysis or triangular fibrocartilage of the wrist. CT is the best imaging tool for evaluating the calcifications, but the MR imaging, especially on the T2-w images, can demonstrate not only the calcifications but also the amount of granulation tissue and fibrosis [6].

Crowned Dens Syndrome

The “crowned dens” syndrome (CDS) is a clinical-radiological entity presenting typically with acute onset of cervical-occipital pain, associated with fever, rigidity and general signs of inflammation, lasting from days to several weeks. The mean age at presentation is 60–70 years, with female prevalence.

The pathologic substrate is frequently associated to crystal deposits diseases, in most cases calcium pyrophosphate dihydrate (CPPD) but also hydroxyapatite (HA). Other articular inflammatory diseases may be associated with the CDS (RA, RA-DISH and other systemic connective

diseases, as Systemic Sclerosis). Other conditions related to the occurrence of CDS are traumas, articular subluxations and tumors.

The syndrome could remain asymptomatic or cause chronic cervical pain and spinal cord compression; the classic onset, represented by a triad of symptoms (headache, fever and morning cervical pain) is aspecific, being related to different conditions, as infectious meningitis or also metastatic cervical spondylitis. Atypical clinical presentations include painful cervicobrachial syndrome (associated with shoulder stiffness and weakness) or occipito-temporal headache (similar to the symptom associated to atypical rheumatic polymyalgia or giant cell arteritis).

Imaging

CT scan represent the diagnostic gold standard: the findings that allow the definition of CDS (in the adequate clinical scenario) are calcifications of all odontoid articular structures (synovial membrane, articular capsule and ligaments); typically the aspect of calcification is narrow and irregular, surrounding the odontoid process (“horseshoe appearance”) with other smaller calcifications located at the apex of the dens surrounding the main calcification (Fig. 3.16).

CT also permit the evaluation of cortical bone, periodontoid calcifications and the presence of other smaller calcifications surrounding the odontoid process: moreover it can depict

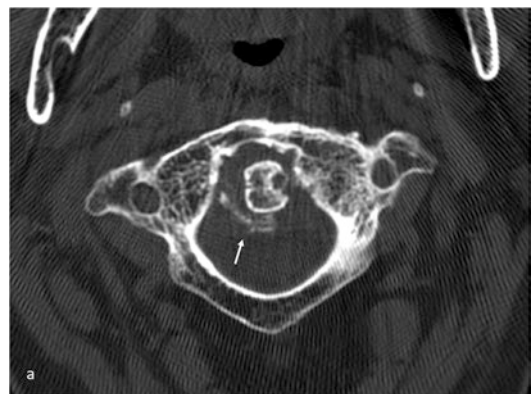


Fig. 3.16 Crowned dens, CT imaging. Axial. Mineralization of transverse ligament of the atlas, more evident in the right side (white arrow)

unknown fractures of the dens. However CT scan has some limitation in assessing CDS when performed tardily after an acute symptomatic attack (because the calcifications may have been reabsorbed or may migrate). This event is more often related to CDS associated with Hydroxy-Apatite Deposition Disease (HADD)-rheumatism [43].

Cranio Cervical Junction Pseudotumor

The retro-odontoid pseudotumor (ROP) represents a non-neoplastic proliferation of soft tissues at the atlantoaxial junction.

Retro-odontoid pseudotumor is commonly associated with atlantoaxial microinstability or subluxation: overtime the mass can determine compressive myelopathy on adjacent spinal cord. The symptoms may be variable, ranging from neck pain (the most frequent), headache and/or neck stiffness to paraparesis and paralysis (in the severe cases).

The retro-odontoid pseudotumor can be associated with several pathologic conditions;

RA is the most common disease associated to the development of retro-odontoid pseudotumor; a variable degree of retro-odontoid soft tissue thickening has been found in up to 83% patients [44], more frequently in patients with known peripheral arthritis; isolated retro-odontoid pseudotumor in this group of patients is rare [45].

The non-rheumatoid conditions related to retro-odontoid pseudotumor, with and without atlantoaxial instability, include: chondrocalcinosis, hemodialysis-associated amyloidosis, chronic odontoid fracture, gout, pigmented villonodular synovitis (PVNS) and ossification of the posterior longitudinal ligament. Other, less frequent conditions related to the growth of mass-like formations in the retro-odontoid region are represented by retro-odontoid synovial cysts, epidural hematoma and/or lipomatosis.

Surgical treatment of local instability is considered the best therapeutic option. Multiple cases reported in literature demonstrated volu-

metric regression of the pseudotumor after surgical stabilization of cranio-cervical junction.

Development of chronic atlantoaxial instability and resulting mechanical stress are treated surgically mostly with posterior fusion (with occipitocervical or atlantoaxial fusion): this procedure is an appropriate surgical strategy for retro-odontoid pseudotumor associated with atlantoaxial subluxation [46].

Kakutani et al. [47] analyzed the surgical outcomes of C1 laminectomy for retro-odontoid pseudotumor without atlantoaxial instability, finding an improvement in all the patients treated and included in the study.

Both Kobayashi et al. and Kakutani et al. studies evidenced that the retro-odontoid pseudotumor that showed higher pre-operative MRI contrast enhancement, thus reflecting an higher neovascularization around the pseudotumor, had higher rates of regression after surgery.

Imaging

Neutral and flexion-extension radiographs are the primary imaging modality to evaluate cervical spine instability, with flexo-extension radiograph recommended in this clinical scenario.

Multidetector computed tomography is useful for identifying bony erosions, fracture, alignment, relationship of the joints and presence of pseudotumor: moreover the CT study easily evaluate the eventual mineralization within the retro-odontoid pseudotumor or in the peri-odontoid ligaments.

MRI represent nowadays the gold standard for the demonstration of retro-odontoid pseudotumor, allowing the identification of early pathological changes in case of early RA and the evaluation of tissue characteristics of the pseudotumor itself (determining the presence of hemorrhage, mineralization, fibrous tissue and, after contrast administration, the vascularity).

Some of the conditions related to the development of retro-odontoid pseudotumor present specific imaging characteristics.

In RA, ROP can show different histologic components (hypervascular, fibrous, or com-

bined), that reflects on different MRI appearance: high signal in T2-weighted images and enhancement in case of hypervascular pannus; intermediate signal intensity on T2-weighted images and absence of post-contrast enhancement in case of hypovascular pannus; and low signal intensity on T1 and T2-weighted sequence, without enhancement in case of fibrous pannus.

In CPPD the MRI signal would be usually low in T1 and variable-heterogeneous in T2-weighted imaging, due to the presence of calcium pyrophosphate dihydrate crystals deposits into hyaline and fibrocartilage.

Hemodialysis-associated amyloidosis can show cystic changes and erosions within the bony structures, better identified by CT.

In PVNS, histologically characterized by infiltrations of mononuclear histiocytes and multinucleated giant cells, the MRI signal is variable and heterogeneous in T1- and T2 weighted imaging, with “blooming” in gradient echo imaging determined by the presence of hemosiderin deposit.

The Gout rarely involves the cranio-cervical junction; the tophus, that can also cause well delineated bony erosions, are characterized by different grades of calcifications that determine a variable signal in MRI, not easily differentiable from a deposit of calcium hydroxyapatite crystals; dual-energy CT can be a useful diagnostic tool, allowing to differentiate between urate and calcific mineralization (that show different attenuation on the 80- and 140-kVp acquisitions).

In OPLL the ossification of posterior longitudinal ligament and its longitudinal extension can be better ruled out with CT, while on MRI the signal of the ossification is the same of the cortex.

Other conditions such as epidural lipomatosis or hematoma show typically high signal in T1-weighted imaging due to the presence of fat tissue and blood clots, respectively. Retroodontoid synovial cysts, related to degenerative changes involving the ligamentous structures, can show non equivocal MRI findings (a structure with fluid signal) if simple, nevertheless the signal may vary in case of complicated cysts [48].

References

1. Pistolesi GF, Bergamo Andreis IA: L'imaging diagnostico del rachide. Ed Libreria Cortina Verona: Verona; 1987.
2. Ross J. Neuroimaging clinics of North America. Philadelphia: WB Sanders; 1995.
3. Maigne JY, Deligne L. Computed tomography follow-up study of 21 cases of nonoperatively treated cervical intervertebral soft disk herniation. *Spine*. 1994;19:189–91.
4. Milligram MA, Rand N. Cervical spine anatomy. *Spine State Art Rev*. 2000;14(3):521–32.
5. Johnson R. Anatomy of the cervical spine and its related structures. In: Torg JS, editor. *Athletic injuries to the head, neck, and face*. 2nd ed. St Louis: Mosby-Year Book; 1991. p. 371–83.
6. Ross JS, Moore KR, Borg B, et al. *Diagnostic imaging: spine*. 2nd ed. Salt Lake City: Amirsys; 2010.
7. Colosimo C, Pileggi M, Pedicelli A, Perotti G, Costantini AM. Diagnostic imaging of degenerative spine diseases. Technical approach. In: *Minimally invasive surgery of lumbar spine*. London: Springer; 2014.
8. Fullenlove T, Williams AJ. Comparative roentgen findings in symptomatic and asymptomatic backs. *Radiology*. 1957;68:572–4.
9. Gehweiler JA, Daffner RH. Low back pain: the controversy of radiologic evaluation. *AJR Am J Roentgenol*. 1983;140:109–12.
10. Wood KB, Popp CA, Transfeldt EE, Geissele AE. Radiographic evaluation of instability in spondylolisthesis. *Spine*. 1994;19:1697–703.
11. Rothman SLG, Glenn WV. *Multiplanar CT of the spine*. Chapters 1–4, p. 1–112, chapters 16–17, p. 477–504. Baltimore: University Park Press; 1985.
12. Hirsch C, Shajowicz F. Studies on structural changes in the lumbar anulus fibrosus. *Acta Orthop Scand*. 1952;22:184–231.
13. Yu S, Haughton VM, Sether LA, et al. Criteria for classifying normal and degenerated lumbar intervertebral discs. *Radiology*. 1989;170:523–6.
14. Virgin WJ. Experimental investigations into the physical properties of the intervertebral disc. *J Bone Joint Surg*. 1951;33:607–11.
15. Nachemson A. Some mechanical properties of the lumbar intervertebral discs. *Bull Hosp Joint Dis*. 1962;23:130–43.
16. Modic MT, Steinberg PM, et al. Degenerative disc disease assessment of changes in vertebral marrow with imaging. *Radiology*. 1988;166:193–9.
17. Giunti A, Laus M. *Le Radicolopatie Spinali*. Bologna: Aulo Gaggi Editore; 1992.
18. Alizada M, Li RR, Hayatullah G. Cervical instability in cervical spondylosis patients. *Orthopäde*. 2018;47:977–85. <https://doi.org/10.1007/s00132-018-3635-3>.

19. Rydman E, Bankler S, Ponzer S, Järnbert-Pettersson H. Quantifying cervical spondylosis: reliability testing of a coherent CT-based scoring system. *BMC Med Imaging*. 2019;19(1):45.
20. Panjabi MM, Krag MH, White AA, Southwick WO. Effects of preload on load displacement curves of the lumbar spine. *Orthop Clin North Am*. 1977;8:181–92.
21. Kirkaldy-Willis WH. The pathology and pathogenesis of low back pain. In: Kirkaldy-Willis WH, editor. *Managing low back pain*. New York: Churchill Livingstone; 1983. p. 23–43.
22. Weyreuther M, Heyde CE, Westphal M, Zierski J, Weber U. *MRI atlas, orthopedics and neurosurgery, the spine*. Heidelberg: Springer; 2007.
23. Kramer J. *Intervertebral disc disease*. 2nd ed. New York: Thieme; 1992.
24. Wiltse LL, Berger PE, McCulloch JA. A system for reporting the size and location of lesions in the spine. *Spine*. 1997;22(13):1534–7.
25. Scott AW. *Magnetic resonance imaging of the brain and spine, vol. 2*. Philadelphia: Lippincott Williams & Wilkins; 2009. p. 1491.
26. Kang Y, Lee JW, Koh YH, et al. New MRI grading system for the cervical canal stenosis. *AJR Am J Roentgenol*. 2011;197(1):W134–40.
27. Yue WM, et al. The Torg-Pavlov ratio in cervical spondylotic myelopathy: a comparative study between patients with cervical spondylotic myelopathy and a nonspondylotic, nonmyelopathic population. *Spine*. 2001;26(16):1760–4.
28. Tsuruda JS, Norman D, Dillon W, et al. Three-dimensional gradient-recalled MR imaging as a screening tool for the diagnosis of cervical radiculopathy. *AJNR Am J Neuroradiol*. 1989;10:1263–71.
29. Takahashi M, Yasuyuki Y, Yuji S, et al. Chronic cervical cord compression: clinical significance of increased signal intensity on MR images. *Radiology*. 1989;173:219–24.
30. Julkunen H, Heinonen OP, Knekt P, Maatela J. The epidemiology of hyperostosis of the spine together with its symptoms and related mortality in a general population. *Scand J Rheumatol*. 1975;4:23–7.
31. Cassim B, Mody GM, Rubin DL. The prevalence of diffuse idiopathic skeletal hyperostosis in African blacks. *Br J Rheumatol*. 1990;29:131–2.
32. Resnick D, Shaul RS, Robins JM. Diffuse idiopathic skeletal hyperostosis (DISH): Forestier's disease with extraspinal manifestation. *Radiology*. 1975;115:513–24.
33. Resnick D, Niwayama G. Radiographic and pathological features of spinal involvement in diffuse idiopathic skeletal hyperostosis (DISH). *Radiology*. 1976;119:559–68.
34. Kuperus JS, de Gendt EEA, Oner FC, de Jong PA, Buckens SCFM, van der Merwe AE, Maat GJR, Regan EA, Resnick DL, Mader R, Verlaan JJ. Classification criteria for diffuse idiopathic skeletal hyperostosis: a lack of consensus. *Rheumatology (Oxford)*. 2017;56(7):1123–34.
35. Cammisa M, De Serio A, Guglielmi G. Diffuse idiopathic skeletal hyperostosis. *Eur J Radiol*. 1998;27(Suppl 1):S7–11.
36. Kuperus JS, Oudkerk SF, Foppen W, Mohamed Hoesein FA, Gielis WP, Waalwijk J, Regan EA, Lynch DA, Oner FC, de Jong PA, Verlaan JJ. Criteria for early-phase diffuse idiopathic skeletal hyperostosis: development and validation. *Radiology*. 2019;291(2):420–6.
37. Resnick D, Guerra J Jr, Robinson CA, Vint VC. Association of diffuse idiopathic skeletal hyperostosis (DISH) and calcification and ossification of the posterior longitudinal ligament. *AJR Am J Roentgenol*. 1978;131(6):1049–53.
38. Hanakita J, Suwa H, Namure S, et al. The significance of the cervical soft disk herniation in the ossification of the posterior longitudinal ligament. *Spine*. 1994;19:412–8.
39. Lee DH, Cho JH, Kim NH, Kim S, Choi J, Hwang CJ, Lee CS. Radiological risk factors for progression of ossification of posterior longitudinal ligament following laminoplasty. *Spine J*. 2018;18(7):1116–21.
40. Doi T, Sakamoto R, Horii C, Okamoto N, Nakajima K, Hirai S, Oguchi F, Kato S, Taniguchi Y, Matsubayashi Y, Hayashi N, Tanaka S, Oshima Y. Risk factors for progression of ossification of the posterior longitudinal ligament in asymptomatic subjects. *J Neurosurg Spine*. 2020:1–7. <https://doi.org/10.3171/2020.3.SPINE2082>.
41. Leone A, Sundaram M, Cerase A, Magnavita N, Tazza L, Marano P. Destructive spondyloarthropathy of the cervical spine in long-term hemodialyzed patients: a five-year clinical radiological prospective study. *Skeletal Radiol*. 2001;30:431–41. *Int Skeletal Soc (ISS)*
42. Nagamachi A, Takahashi M, Mima N, Adachi K, Inoue K, Jha SC, Nitta A, Morimoto M, Takasago T, Iwame T, Wada K, Tezuka F, Yamashita K, Hayashi H, Miyagi R, Nishisyo T, Tonogai I, Goto T, Takata Y, Sakai T, Higashino K, Chikawa T, Sairyo K. Radiographic changes of cervical destructive spondyloarthropathy in long-term hemodialysis patients: a 9-year longitudinal observational study. *J Med Investig*. 2017;64(1.2):68–73.
43. Scutellari PN, Galeotti R, Leprotti S, Ridolfi M, Franciosi R, Antinolfi G. The crowned dens syndrome. Evaluation with CT imaging. *Radiol Med*. 2007;112(2):195–207. English, Italian
44. Stiskal MA, Neuhold A, Szolar DH, et al. Rheumatoid arthritis of the craniocervical region by MR imaging: detection and characterization. *Am J Roentgenol*. 1995;165(3):585–92.
45. Del Grande M, Del Grande F, Carrino J, Bingham CO, Louie GH. Cervical spine involvement early in the course of rheumatoid arthritis. *Semin Arthritis Rheum*. 2014;43(6):738–44.
46. Kobayashi K, Imagama S, Ando K, Nishida Y, Ishiguro N. Post-operative regression of retro-odontoid pseudotumors treated with and without fusion. *Eur Spine J*. 2018;27(12):3105–12.

-
47. Kakutani K, Doita M, Yoshikawa M, Okamoto K, Maeno K, Yurube T, Sha N, Kurosaka M, Nishida K. C1 laminectomy for retro-odontoid pseudotumor without atlantoaxial subluxation: review of seven consecutive cases. *Eur Spine J.* 2013;22(5):1119–26.
48. Shi J, Ermann J, Weissman BN, Smith SE, Mandell JC. Thinking beyond pannus: a review of retro-odontoid pseudotumor due to rheumatoid and non-rheumatoid etiologies. *Skelet Radiol.* 2019;48(10):1511–23.